nature protocols

REVIEW ARTICLE

https://doi.org/10.1038/s41596-020-0313-9

Check for updates

Tutorial: guidance for quantitative confocal microscopy

James Jonkman[1✉], Claire M. Brown[2], Graham D. Wright[3], Kurt I. Anderson[4] and Alison J. North[5]

When used appropriately, a confocal fluorescence microscope is an excellent tool for making quantitative measurements in cells and tissues. The confocal microscope's ability to block out-of-focus light and thereby perform optical sectioning through a specimen allows the researcher to quantify fluorescence with very high spatial precision. However, generating meaningful data using confocal microscopy requires careful planning and a thorough understanding of the technique. In this tutorial, the researcher is guided through all aspects of acquiring quantitative confocal microscopy images, including optimizing sample preparation for fixed and live cells, choosing the most suitable microscope for a given application and configuring the microscope parameters. Suggestions are offered for planning unbiased and rigorous confocal microscope experiments. Common pitfalls such as photobleaching and cross-talk are addressed, as well as several troubling instrumentation problems that may prevent the acquisition of quantitative data. Finally, guidelines for analyzing and presenting confocal images in a way that maintains the quantitative nature of the data are presented, and statistical analysis is discussed. A visual summary of this tutorial is available as a poster (https://doi.org/10.1038/s41596-020-0307-7).

Confocal microscopes offer a modest advantage over regular 'widefield' (epifluorescence) microscopes in resolution, but their main advantage is the ability to generate high-contrast images through optical sectioning. In a widefield microscope, the acquired images are a superposition of sharp features from the focal plane and blurry features from outside of the focus. A confocal microscope blocks the latter, resulting in a sharp image from the focal plane alone (Fig. 1a,b). With a high-resolution objective lens, a confocal microscope can generate optical sections thinner than 1 µm without having to physically slice the sample. It can therefore be used to quantify the intensities and investigate the spatial arrangement of fluorescent molecules with high precision, which is useful for assigning the localization of molecules to specific cellular compartments or assessing the colocalization of different molecules. A single confocal image (or 'slice') may be sufficient for quantification if it is representative of the entire thickness of the sample, but one can also take a series of confocal images while changing the focus to produce a 3D dataset (or 'z-stack'), enabling the reconstruction and quantification of the entire sample volume (Fig. 1c,d).

The essential component common to all confocal microscopes is one or more strategically placed pinhole apertures. Figure 2a shows a schematic of the main components and the lightpath in the classic confocal laser-scanning microscope (CLSM). A laser beam is focused into a specimen, where it excites fluorescent molecules throughout the entire cone of illumination. The light emitted by these excited fluorescent molecules (i.e., fluorescence) is collected by the objective lens and focused by a second lens through a carefully aligned pinhole. The pinhole ensures that only fluorescence that originates at the focal point is captured by the detector; fluorescence emission from above or below the focal plane is blocked. The name 'confocal' derives from the position of the pinhole(s) in the microscope's lightpath, in a CONjugate FOCAL plane with the sample. As the CLSM collects fluorescence from only one focal point at a time, scanning mirrors are used to sweep the laser beam across the specimen, generating an image pixel by pixel. Since you typically must dwell for ~1 µs on each pixel to collect enough fluorescence, it takes ~1 s to generate a modest 1,024 × 1,024 pixel (1 megapixel) image. To capture fast dynamics in live specimens, small regions of interest can be scanned, or a different confocal geometry might be needed. One such alternative is a spinning-disk confocal microscope (SD), which illuminates the sample using an array of pinholes arranged in a special pattern on a disk, creating hundreds of focused beams (Fig. 2b). The fluorescence is then collected back through the pinholes (creating the optical section) and detected using a digital camera—effectively parallelizing multiple confocal lightpaths. The disk spins to rapidly sweep the pattern of

[1]Advanced Optical Microscopy Facility (AOMF), University Health Network, Toronto, Ontario, Canada. [2]Advanced BioImaging Facility (ABIF), McGill University, Montreal, Quebec, Canada. [3]A*STAR Microscopy Platform (AMP), Skin Research Institute of Singapore, A*STAR, Singapore, Singapore. [4]Crick Advanced Light Microscopy Facility (CALM), The Francis Crick Institute, London, UK. [5]Bio-Imaging Resource Center, The Rockefeller University, New York, NY, USA. ✉e-mail: james@aomf.ca

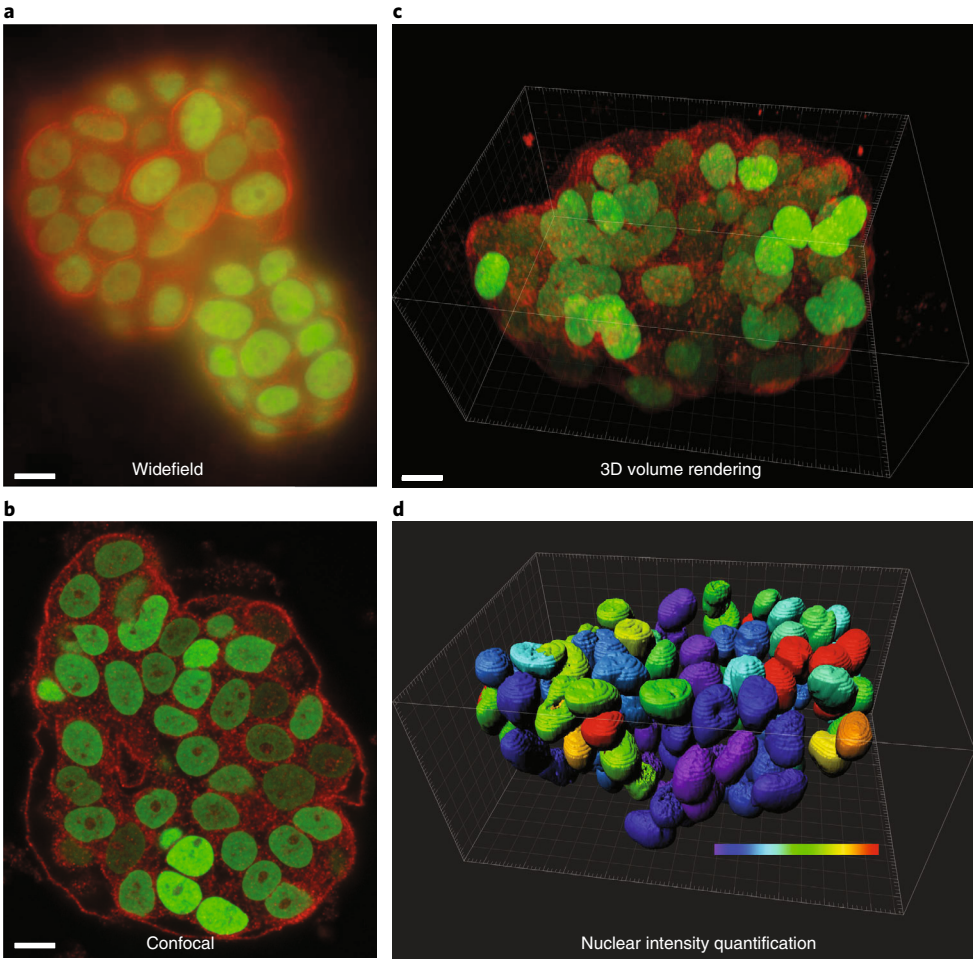

Fig. 1 | Quantitative confocal microscopy example. a and **b**, Widefield image (**a**) and a single confocal image slice (**b**) of an organoid expressing a fluorescently labelled nuclear protein (green: H2B-Venus) and with a fluorescent membrane probe (red: DiI, Thermo Fisher)[96]. **c**, Confocal 3D volume rendering of the organoid. **d**, 3D quantification of the mean nuclear intensities with color coding from 9,000 counts (violet) to 30,000 counts (red). Scale bars = 10 μm. Cells courtesy of Hui Wang (Princess Margaret Cancer Centre, Toronto, ON, Canada). Images in **a** and **b** used with permission from the Journal of Biomolecular Techniques (JBT), ©Association of Biomolecular Resource Facilities, http://www.abrf.org.

laser beams across the specimen to image the entire field of view. Since SDs are usually optimized for speed, they are sometimes less well suited for applications where image quality, rather than speed, is paramount. The relative advantages and disadvantages of different confocal modalities are discussed in more detail below in 'Choosing the right microscope'.

Despite being quite sophisticated, it is relatively straightforward to snap pictures on a modern confocal microscope. However, generating quantitative image data requires thoughtful planning and careful execution at all stages of the experiment. Some applications have a clear requirement for quantification, such as measuring the change in expression levels of a fluorescently labeled protein. In other cases, the reason for requiring quantification may be less obvious. For example, it is tempting to assume that preliminary experiments will not require quantification; yet quantitative images are necessary even for reliable qualitative comparisons ('sample A is brighter than sample B'). Quantitative imaging is also necessary to apply a consistent intensity threshold during cell counting and segmentation and measuring morphology of structures. Ultimately, most experiments that use confocal microscopy require (or benefit from) quantitative acquisition to produce meaningful data.

Quantitative confocal microscopy involves rigorous specimen preparation, careful selection of an appropriate microscope for a given application, stringent microscope set up and operation in a way that enables equal and fair assessment of control and experimental conditions. Common pitfalls such as photobleaching and cross-talk must be avoided. Care must be taken to avoid bias and ensure that the measured differences are statistically meaningful. All image processing and analysis steps must be performed cautiously and with integrity. Unfortunately, even the latest confocal microscopes may suffer from instrumentation problems that can dramatically affect their ability to generate quantifiable data[1]. Illumination intensity may vary substantially from the center of the image to the periphery (often as high as 40%). Focus drift often plagues time-lapse imaging (a 0.5-μm change in focus over 5 min is typical) and can create the false impression that sample intensity is changing. Particularly troubling are laser power fluctuations that can

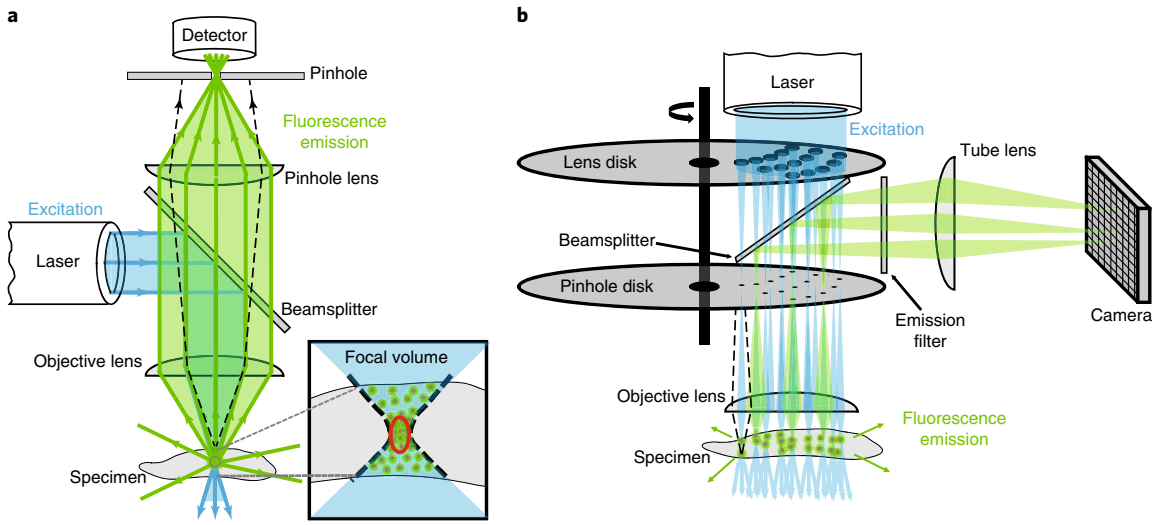

Fig. 2 | Principles of confocal microscopy. a, In the CLSM, a laser beam is focused into a specimen, where fluorescent molecules are excited throughout the entire cone of illumination. Photons emitted by fluorescent molecules in the focus (red oval) are imaged through a pinhole onto a detector. Light emitted by fluorescent molecules located outside the focus, such as the cell surface, is not focused through the pinhole and therefore does not reach the detector (black dashed lines). **b**, In the SD, a laser beam hits a lens disk that splits the beam up into ~1,000 smaller beams, which pass through a matching pinhole disk and are focused into the specimen. Fluorescent molecules are excited throughout the focal volume and across the field of view of the specimen as the rotating disk sweeps the pattern of laser beams (the emitted light path is shown in green). Fluorescence generated from the many focal points passes back through the pinholes and is reflected by a beamsplitter to a digital camera. Light emitted by fluorescent molecules located outside the focus (black dashed lines) does not pass through the pinhole disk and is not detected.

alter the intensity by 10–25% over a typical 3-h imaging session. Other unexpected pitfalls could include variability in fluorophore emission depending on the sample mounting media and changes in image analysis processes with software updates. The confocal microscope user must navigate this quagmire of unexpected issues using a careful, step-by-step approach to ensure that each link of the image acquisition and analysis chain is trustworthy and reproducible. Future hardware improvements by manufacturers could also be greatly beneficial towards enabling reliable quantitative confocal microscopy.

General considerations for preparing samples for quantitative fluorescence microscopy

Sample preparation is one of the most critical steps in any fluorescence microscopy experiment, leading to the microscopists' motto of 'garbage in = garbage out'. The higher the performance of the microscope, the more likely it is to reveal inadequate sample preparation. All microscopy work benefits from optimizing the lightpath between the objective lens and the focal plane in the sample. A particularly insidious problem is spherical aberration, which leads to image blur, particularly in the z-axis, and loss of signal intensity[2]. Spherical aberrations result primarily from the use of inappropriate coverslips and refractive index (RI) mismatch between the microscope objective immersion medium and the sample[3] (more details in Setting up the microscope). Modern objective lenses are designed to be used with 170-µm-thick coverslips, closely approximated by #1.5 coverslips, which typically range between 160 and 190 µm in thickness. High precision versions (#1.5H) with only ±5-µm variance are now also available (e.g., Carl Zeiss, Marienfeld GmbH, and Thorlabs). For high-resolution imaging, the use of any other coverslip thickness requires the use of an objective with an adjustable correction collar. It is best to grow cultured cells directly on the coverslip to minimize the distance between the coverslip and the specimen. Multi-well microscope slides with removable gaskets can be problematic if there is any kind of 'spacer' or residual substance left on the slide after removing the gasket. Dishes or chambers with a #1.5 glass coverslip bottom are very useful when working with live cells on an inverted microscope (see below).

Preparing fixed cells and tissues

For fixed samples, the most critical sample preparation steps are fixation, permeabilization, labeling and mounting, all of which will be discussed in detail in the following sub-sections. In addition, tissues require sectioning at an appropriate thickness. For widefield microscopy, sections are generally 4–10 µm thick, but for confocal microscopy 10–40 µm is more common. Antibody and fluorophore penetration beyond 40 µm is challenging[2] and may require modified labeling protocols or perfusion of probes. Tissue-clearing techniques can be used to render the tissue more transparent for imaging of thicker sections or even whole organs[4].

Fixation

There is no such thing as a 'standard' fixation protocol: fixation must be optimized for every cell or tissue type. Fixation methods can be chemical or physical. In biomedical research, chemical fixations, typically using cross-linking approaches (aldehyde fixation) or precipitation methods (methanol, ethanol, or acetone) are most commonly used[5]. Physical methods such as high-pressure freezing, more common in electron

microscopy (EM), offer superior preservation of some samples, including worms and yeast[6]. In chemical fixation, the trick is to address what is known as the immunocytochemical compromise—sufficient cross-linking is necessary to preserve morphological details, but too many cross-links can reduce antigenicity and prevent antibody penetration. Hence, fixation must be optimized for each target structure and antibody. Very stable tissue structures (e.g., cell-cell junctions) are easily retained in place, such that gentle methanol fixation may suffice for the purposes of identification[7], while other tissue components, such as soluble proteins, require more stringent fixatives such as aldehydes. The choice of imaging approach will also dictate the method to be used, since EM and even super-resolution microscopy approaches will reveal more subtle changes to the tissue architecture than lower-resolution approaches. Thus, while formaldehyde (FA) fixation is typically used in most fluorescence microscopy protocols, the bivalent cross-linker glutaraldehyde is commonly added in EM protocols. Importantly, certain cellular structures, such as microtubules, are also best preserved for fluorescence imaging using low concentration glutaraldehyde fixatives[5]. Be aware of the different sources of FA: formalin solution, commonly used by pathologists, also contains methanol; hence, FA prepared in pure solution from paraformaldehyde powder is generally superior to methanol formalin solution for immunocytochemistry. The duration and temperature of fixation must also be optimized. For antibodies or structures that do not withstand aldehyde fixation well, it can be helpful to try fixation using ice-cold methanol, acetone or ethanol. Conversely, the fixation of cytoskeletal structures can often benefit from warming the fixative (e.g., 37 °C), particularly for mammalian cells, to prevent a cold shock to the cells and disassembly of the cytoskeletal structures. Note that polyclonal antibody staining is generally more resistant to chemical fixation than staining with monoclonal antibodies, since they detect multiple epitopes[8]. Researchers should refer to literature on their specific tissues, structures and molecular targets of interest to determine the optimal fixation protocol for their experiments, and should also be aware of new, improved tissue preservation methods that are constantly being developed[9,10] and should be tested.

Permeabilization

Antibodies and fluorophores are generally unable to penetrate the plasma membrane and reach the cytoplasm, unless detergents are used to make holes in the membranes. The permeabilization regime and detergent choice must be optimized. Some structures are better revealed by a brief permeabilization step prior to or during fixation, but it is important to realize that soluble proteins will be removed during this process. If soluble proteins are the target of the staining, this is obviously problematic, but if other structures (e.g., focal adhesions) are the target, permeabilization during fixation can remove cytosolic proteins, thereby reducing background signal and improving image contrast. In order to retain soluble proteins, however, most protocols either fix first, or fix and permeabilize simultaneously. We recommend trying combinations of different steps to determine the best results for the target of interest. Insufficient permeabilization of tissue sections can lead to poor antibody penetration only into the top and/or bottom of the tissue, while too much permeabilization can lead to loss or artifactual redistribution of the target[11]. Triton-X is a harsher detergent than saponin, which interacts selectively with membrane cholesterol, producing small holes in the plasma membrane without affecting cholesterol-poor membranes of the mitochondria and the nuclear envelope[12]. However, saponin's effects are reversible, so it must be included in all solutions during the entire labeling procedure. Finally, when labeling surface proteins, it should be noted that the small amount of methanol in formalin can cause some cell permeabilization and allow labeling also of internal structures.

Labeling

The next step is to select an appropriate labeling method to specifically target and visualize the structure of interest. This could involve antibody staining or a direct labeling approach (the latter may negate the need for permeabilization). Genetic approaches, fluorescent proteins (FPs) or tags such as SNAP-tags and HALOtags[13], have been increasingly used over the past decades, but antibody approaches are still prevalent and useful for verifying the localization of genetically tagged proteins to the correct cellular structures. The use of nanobodies to couple more photostable organic dyes to genetically expressed FPs is particularly useful for super-resolution microscopy techniques[14] but can also be applied for confocal microscopy. Companies also sell reagents for tagging specific cellular structures, such as DNA dyes for the nucleus or fluorescent markers for specific organelles (membranes, lysosomes, mitochondria, etc.)[15,16].

There is no such thing as a 'standard' immunolabeling protocol for cells or tissues: entire books have been written on this topic alone[8]. Blocking steps (e.g., with BSA or serum) should be introduced when required (inevitably for tissues, often for cell monolayers), to minimize non-specific binding of primary or secondary antibodies that can lead to background fluorescence, or to block endogenous enzyme activity when using enzymatic labeling approaches. Appropriate antibody concentrations must be established, as well as the optimal duration and temperature of labeling. Although counter-intuitive, reducing antibody concentrations often leads to better staining as specific binding is retained at the expense of non-specific binding. The optimal duration can vary widely from 20–30 min for cultured cells to hours or even days for tissue sections or cleared organs. If labeling at room temperature results in a high level of background signal, incubation of the sample with primary antibody overnight at 4 °C may increase specificity. Incubation times with secondary antibodies (typically 30 min to 1 h) can be reduced to lower nonspecific background. Sufficient washing steps are also critical, with many, shorter washes being superior to a couple of long ones. Also note that total labeling and washing times for weakly fixed tissue or cells should be minimized to prevent loss of cellular components from the sample. Finally, a variety of controls are essential for both primary and secondary antibodies, including minus primary antibody and isotype controls[8]. Positive controls, such as overexpression of the protein of interest or expression in a cellular system that does not express the protein

of interest, are often as important as negative controls, especially when the quality of the primary antibody is unknown[17,18]. The ideal negative control for primary antibody staining is generally knockdown of the protein of interest to show loss of all antibody staining[19].

Use the brightest and most stable fluorophores available. Microscopists should avoid many common flow cytometry dyes, such as fluorescein and phycoerythrin, that are prone to rapid photobleaching. Fluorescent tags designed specifically for microscopy are generally superior, such as the Alexa Fluor, Cyanine, DyLight and Silicone Rhodamine dyes, and the non-commercial Janelia Fluor dyes. Fluorophore wavelengths must be carefully chosen. Several companies (such as Chroma, Semrock, Omega and Thermo Fisher) offer online spectra viewers that display excitation and emission spectra of fluorophores, combined with filter sets and excitation sources to help match them to the available lasers/filters on the microscope and minimize spectral overlap between multiple probes. If the signal intensities of different fluorophores are balanced, most confocal microscopes can easily image four fluorophores without significant excitation or emission cross-talk. Most modern point-scanning confocal systems are capable of spectral unmixing, tempting users to label with five or more fluorophores at once. However, this complicates the sample preparation, imaging and analysis; so consider whether all five components need to be labeled at the same time, or whether the same information can be obtained by labeling two successive samples. When tissue autofluorescence is a major problem, avoid shorter wavelength (blue/green-emitting) dyes. However, this must be balanced with the need for high resolution, as long wavelength dyes (e.g., near infrared) will reduce the achievable resolution (Fig. 3). Chromatic aberration, where different wavelengths of light coming from the same point in the sample are focused to slightly different points in the image, is most problematic when combining blue-emitting dyes with other colors[2]. Certain objective lens types (e.g., Plan Apochromat) are better corrected than others, but very few are well corrected across the entire spectrum. Chromatic aberration will critically affect any colocalization analysis and should be measured and corrected for using multicolor microspheres (beads)[20].

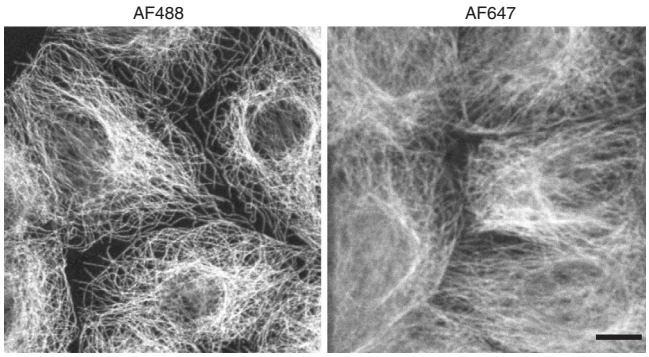

Fig. 3 | Effect of wavelength on resolution. MDCK-II epithelial cells (RRID: CVCL 0424) were fixed in ice-cold methanol and stained using a monoclonal anti-tubulin antibody (RRID: AB_378784) followed by secondary antibodies conjugated to either Alexa Fluor 488 (AF488) or Alexa Fluor 647 (AF647; Thermo Fisher). Single optical sections were acquired using a Leica SP8 confocal microscope and a 40×/1.1 NA water immersion objective, with an optical zoom of 4 and the confocal pinhole set at 1 AU at 580-nm emission. The fact that resolution is inversely proportional to wavelength is well known in theory, but rarely considered in practice. Far-red emitting dyes, such as AF647, have become increasingly popular in recent years due to lower autofluorescence in this region of the spectrum and their compatibility with certain super-resolution techniques such as stochastic optical reconstruction microscopy (STORM) and stimulated emission depletion (STED) microscopy. However, shorter wavelength dyes (blue- or green-emitting) prove significantly better for imaging fine structures at high resolution on confocal microscopes. Scale bar = 10 μm.

Sample mounting

Sometimes researchers unwittingly ruin their carefully prepared specimens at the final hurdle of mounting the sample. Inappropriate mountants cause problems in two major areas: loss of 3D information and loss of signal. Glycerol-based or uncured mountants will preserve 3D information (critical for morphology and colocalization analysis) better than hardening mountants, which cause the sample to flatten. Mountants designed to give a certain refractive index after hardening (such as Prolong Diamond) can be prevented from curing to preserve 3D structure by immediately sealing around the entire coverslip edges using a quick-drying nail polish (colored quick-dry types are the best, as it is difficult to spot gaps with clear polish), though clearly this will alter the final RI. It is important to know whether the antifade reagent included in the mountant is compatible with the fluorophores used. No one anti-fade works with all fluorophores, and an inappropriate anti-fade may drastically reduce signal intensity (Fig. 4) as well as proving ineffective against photobleaching. For example, Vectashield, which preserves fluorescein optimally and is compatible with many other blue/green dyes, markedly reduces fluorescence from some far red dyes, including Alexa Fluor 647[21]. Published information on the incompatibility of specific antifade reagents with different fluorophores is scarce. Thus, test different mountants on your chosen dyes and compare the results empirically. Sometimes completely inexplicable results will be obtained (Fig. 4) that are often incorrectly attributed to poor antibody labeling. Do not use a mountant that contains DAPI as a nuclear counterstain, as this increases background fluorescence. Instead, perform DNA staining as a separate step before mounting. Be aware that DAPI staining can also photo-convert to give green fluorescence with extended UV excitation[22].

Quality control

Before using the confocal microscope, check to see if the sample preparation was successful for all fixed samples on a widefield fluorescence microscope. Check that negative controls lack fluorescence and that the staining of positive controls is bright and specific. A confocal microscope cannot remove non-specific staining; nor will it increase signal brightness. In fact, signal intensity often appears weaker on the confocal microscope since emitted light is acquired only from a thin optical section, rather than the entire specimen thickness. However, the background and autofluorescence are typically reduced with a confocal microscope, thanks to optical sectioning and to the ability to select narrow-band emission filters or tune the

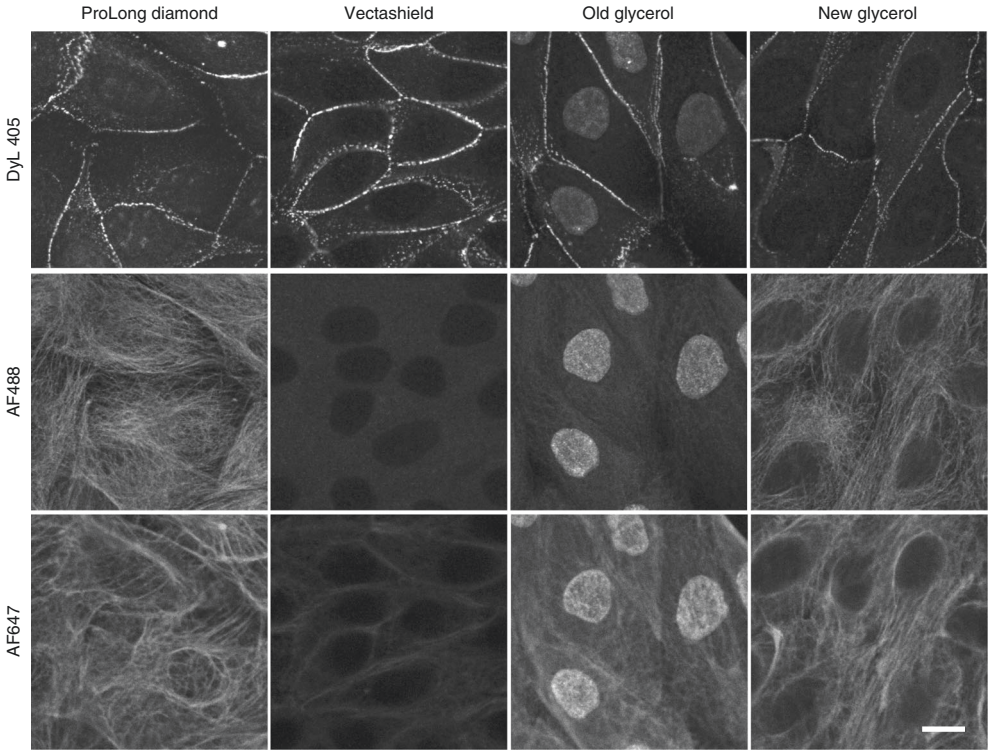

Fig. 4 | Effect of mounting medium on confocal images of fixed cells. MDCK-II epithelial cells (RRID: CVCL 0424) were fixed in ice-cold methanol and triple-stained by indirect immunolabeling using antibodies against the following: desmoplakin (DyLight 405, Jackson Immunoresearch Laboratories), top row; tubulin (Alexa Fluor 488, Thermo Fisher), middle row; cytokeratins (Alexa Fluor 647, Thermo Fisher), bottom row. Triple-labeled coverslips were then mounted using the following: ProLong Diamond (uncured; Thermo Fisher), first column; Vectashield (Vector Laboratories), second column; 100% glycerol (Fisher), third column; a second bottle of 100% glycerol (Fisher), fourth column. Images (single optical sections) were acquired on a Leica SP8 confocal microscope using a 40×/1.1 NA water immersion objective and a sequential track for exciting blue, green and far-red emitting dyes. The same tube containing all three primary antibodies was used for all 12 coverslips, as well as the same tube containing the combined secondary antibodies. Coverslips mounted using ProLong Diamond or the second bottle of glycerol showed the expected localization of each target antigen. However, Vectashield and the first bottle of glycerol produced unexpected effects: Vectashield preserved the DyLight 405 signal well but led to a strong reduction in the initial intensity of AF647, consistent with prior data. However, the AF488 signal, which is typically compatible with Vectashield, was completely quenched. The experiment was repeated twice more, using a second, brand-new bottle of Vectashield as well as two different AF488-conjugated secondary antibodies, but the results were consistent. The first bottle of glycerol led to a different surprise in the form of strong nuclear staining, presumably caused by some contamination. These results are presented not to suggest that the users should avoid the use of Vectashield or glycerol as mountants but to urge caution in assuming that any unexpected or negative staining results must be the result of the antibody per se: it is important to confirm unexpected results through careful control of reagents. Scale bar = 10 μm.

spectral detection. Finally, check samples for antibody precipitates and for strange cellular morphology that could indicate poor fixation or unhealthy cells (e.g., rounding up or blebbing)—a transmitted light (brightfield/phase contrast/differential interference contrast (DIC)) image can help with this assessment. If the sample is suboptimal, start again.

Preparing live cells

Live cell work avoids many of the concerns of fixed-sample preparation listed above, but introduces its own challenges: most notably, how to label structures or molecules of interest and image them without compromising cellular viability or disrupting the complex machinery of the cell[23,24].

Fluorescent protein labeling

With an overwhelming number of FP variants now available (https://www.fpbase.org/)[25], one must carefully select the most appropriate ones according to the microscope's specifications (e.g., lasers and filters), the approach being used (e.g., time-lapse imaging, multi-color, photoactivation, etc.) and the protein, cellular compartment or even the specific organism being studied[26,27]. While the latest super-bright FP variants may appear tempting, the problem of fluorescent protein aggregation[28] or mislocalization may render the tried and tested older FPs, such as EGFP, the best choice for many studies. Ongoing searches of the most recent literature are essential for appropriate probe selection. FPs can be introduced into cells using transient transfections with lipid-based reagents (e.g., lipofectamine or effectine) or, for harder-to-transfect cells (e.g., primary cells, epithelials cells and neurons), electroporation or viral vectors. The timing of each step, reagents, buffers, etc. must be carefully tested for any of these protocols to maximize expression efficiency while ensuring that cell health is not compromised. It is important to monitor fluorescent protein expression levels and adjust experimental conditions or plasmids (e.g., use less-efficient promoters) to reduce the possibility of overexpression artifacts. Cells can be left in selection media for an extended

period of time (2–3 weeks) to develop stable cell lines and sorted using FACS to isolate cells with appropriate levels of expression. FPs are not very bright or photostable, so genetic tags such as SNAP and HALO, which enable the use of optimized fluorescent dyes, are particularly suitable for light-intensive applications such as super-resolution approaches[13,29–32].

Vital dye labeling

There is an ever-growing arsenal of vital dyes available for labeling entire cells (e.g., for tracking) or organelles. Most dyes can simply be added to live cells from a stock solution and incubated for 5–10 min. Adding any dyes to live cells will inevitably cause perturbations to the cellular physiology and interfere with normal function, so dye concentrations must be minimized. When labeling DNA for long-term imaging experiments, avoid dyes that intercalate into the DNA (e.g., Hoechst and DRAQ5). Either FP-labeled histones or SiR-Hoechst can be used without noticeably affecting cell division for some cell types. Many small molecule dyes such as MitoTrackers (to label mitochondria) can be phototoxic, so they should be used at minimal concentrations for longer experiments. In our experience, most dyes can be diluted hundreds of times lower than suggested in manufacturer protocols. Minimize cell stress by finding the lowest dye concentration that still provides adequate signal to visualize the structures of interest.

Live-cell imaging dishes and chambers

Live-cell imaging can be conducted on standard thick-bottomed plastic tissue culture plates using long-working-distance (LWD) lenses but at the cost of sensitivity and resolution. This can be well suited for transmitted light (e.g., phase contrast) cell tracking, cell counts or visualization of cell morphology, but is less suitable for confocal fluorescence applications. Choose #1.5-thickness coverslip-bottom chambers or dishes that enable the use of higher numerical aperture (NA) (>0.5) objective lenses. These range from 35-mm dishes (e.g., MatTek, Wilco and World Precision Instruments) and 2-, 4-, or 8-well chambers (e.g., Labtek, Ibidi and Eppendorf) to devices for chemotaxis and flow experiments (e.g., Ibidi). Multi-well (24-, 96-, and 384-well) plates are also available with glass coverslip bottoms (e.g., Corning, Eppendorf, Ibidi and PerkinElmer). Particularly sensitive cell types, such as stem cells or neuronal cultures, may not adhere well to glass substrates. In this case, coat dishes with, for example, polylysine, collagen or fibronectin (or purchase them pre-coated). Alternatively, optical-quality polymer dishes (Ibidi) can be used, but ensure that they are compatible with the immersion media, as some immersion oils can dissolve the plastic, causing damage to expensive objectives and spills of media. Cells may also be grown on 25-mm-diameter round coverslips and assembled into reusable chambers such as the Attofluor cell chamber (Thermo Fisher) or Chamlide CMB (Live Cell Instruments); however, these may be more prone to leaking compared to manufactured chambers and dishes.

Quality control

Live samples must be healthy before and during imaging: any cell stress will affect the behavior of the cells and add to problems of phototoxicity during imaging. Even the motion and temperature changes associated with transporting cells (e.g., across campus or between buildings) can induce significant stress: consider incubating the cells for a few hours near the microscope before beginning an experiment. Inspect cells for normal morphology, proliferation and minimal cell death even before starting live-cell experiments and consider controls to assess the impact of the imaging you are undertaking. It is best to compare transmitted light images of a separate sample of untreated cells with images of the stained samples as a reference to demonstrate 'normal' cell morphology.

Choosing the right microscope

There is a wide diversity of 2D and 3D fluorescence microscopes available, each with its own advantages and disadvantages. Often a correlative approach, applying several techniques to address the question from different perspectives, is required. Avoid the pitfall of 'the previous student in the laboratory used this microscope; therefore, I should use this microscope'. How, then, should one decide which microscope is best suited to the current experiment?

Start by consulting one of the increasing number of microscopy core facilities[33], where you may find everything from slide scanners and high-end widefield microscopes to confocal (both CLSMs and SDs), multiphoton and super-resolution microscopes. Core facility staff have extensive experience matching researchers' needs to the most suitable microscope. The increasing prevalence of networks of microscopy experts and nationwide/regional infrastructures (e.g., BioImaging North America, BioImaging UK, Canada BioImaging, EuroBioImaging and SingaScope, to reference just the authors' regional networks) has further broadened the selection and access to the relevant expertise.

When selecting a microscope, the key question is 'What is the biological question and what must you measure to answer it?'. Consider the following factors:

- Sample viability: Is the sample alive or fixed? In fixed-cell imaging, fluorophores can photobleach (especially during acquisition of high-resolution z-stacks), and in live-cell imaging, fluorescence excitation also leads to phototoxicity, reducing sample viability in both cases[34]. Choose a technique and microscope configured to be light efficient and sensitive, enabling excitation intensity and duration to be kept to a minimum. Researchers must provide evidence that cells remain viable during and after imaging, for example, through the maintenance of normal morphology and activity, or constant cell division rates[35]. Inverted microscopes are often best suited for live-cell imaging chambers to control environmental conditions including sterility, temperature, CO_2 and humidity.
- Speed: For live-cell imaging, the speed of image acquisition must match the dynamics of the process being studied[34]. Even with fixed samples, acquisition speeds can become important when capturing many thousands of images (e.g., for an image-based screen), large 3D z-stacks or very-high-resolution images. Higher sensitivity instruments can enable faster acquisition without increasing the excitation light intensity. A typical confocal acquisition time is hundreds of milliseconds to several

seconds per fluorophore channel, but modern instruments can be equipped to capture hundreds of images per second for more rapid data collection and for visualizing rapid dynamic processes (e.g., resonant scanning or SD with a fast scientific complementary metal oxide semiconductor (sCMOS) camera).

- Resolution: How small are the features that need to be resolved? The lateral (x-y) resolution of a fluorescence microscope depends on the wavelength (λ) of light and on the NA of the objective lens[36]. Rayleigh's criterion is a rule of thumb for estimating the smallest features that can be resolved laterally:

$$R_{xy} = \frac{1.22\lambda}{2NA} \quad (1)$$

For example, with a high-NA oil immersion objective (NA = 1.4), one can distinguish structures labeled with green fluorophores (λ = ~500 nm) with ~200-nm lateral resolution. Axial (depth, or 'Z') resolution is about two to three times worse than lateral resolution (~400–600 nm in this example).

- Contrast: The ability to 'see' features of interest against the background is vital. Confocal microscopes and related optical sectioning techniques lower the background by excluding out-of-focus light, thereby providing better contrast.
- Depth penetration: Due to absorption and scattering in most biological specimens, depth penetration is generally limited to 50–100 μm for confocal microscopes, and perhaps twice that for multiphoton excitation (see 'Alternative optical sectioning methods'), unless tissue-clearing techniques are employed[4]. Shorter wavelength light (blue/green) experiences higher absorption and scattering than do longer wavelengths[37], so choose red or far-red fluorophores for deeper imaging, though at the cost of resolution (Fig. 3).

Every microscope comes with trade-offs between these parameters. For example, there is often a tendency to prioritize higher image resolution inappropriately. In a higher-resolution image, each pixel captures a smaller area, resulting in less signal per pixel. This may require increasing the excitation light intensity or pixel dwell time, thereby increasing photobleaching and phototoxicity or decreasing the acquisition speed. Higher-resolution images are also larger, requiring more storage space. The goal is to have the appropriate level of resolution to answer the question at hand. In Fig. 5a, the parameters listed above are plotted on the axes of radar plots to visualize how different microscopy techniques perform relative to each other. These are generalized examples—the actual performance of each microscope depends on its exact configuration and settings (Fig. 5b). Nevertheless, these microscopy techniques will be examined one by one to offer guidance.

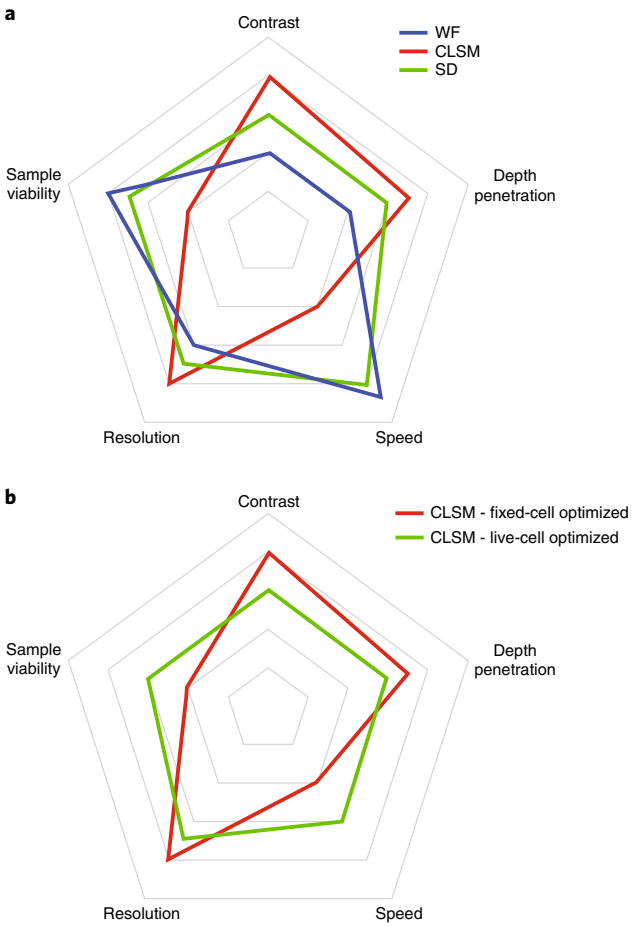

Fig. 5 | Comparing inter-related key instrument performance parameters of different microscopy techniques and configurations. When choosing between different microscopy techniques, it is important to consider how their relative performance attributes, their strengths and weaknesses, make them more or less suitable for a particular experiment. Here, we have limited ourselves to five key parameters (contrast, depth of penetration, speed, resolution and sample viability), although your experimental needs may require you to consider others too (e.g., noise). **a**, The relative performance of typical WFs, SDs and CLSMs are compared with the outer position indicating the best performance for that attribute. It is important to remember that microscopes can be configured differently to optimize for a particular parameter (or combination of parameters), either through the hardware choices or the software settings. **b**, This panel illustrates that the same CLSM instrument can be optimized for either contrast or live-cell imaging, but this comes at the expense of other performance parameters—it is always a trade-off.

Widefield (WF) fluorescence microscope

When imaging a cell monolayer, a well-equipped modern WF microscope may actually be the most suitable choice. Widefield microscopes are highly light efficient and therefore preserve sample viability better than most confocal microscopes. Newer sCMOS digital cameras have high resolution (i.e., they have a large number of small pixels) and are incredibly fast, capable of capturing hundreds of images per second given sufficient signal. The lack of optical sectioning results in relatively poor contrast and depth penetration, prohibiting the discrimination of signal arising from different structures that are in close proximity in the axial (depth) direction (e.g., nucleus and plasma membrane). This renders widefield microscopy generally unsuitable for colocalization analysis[38,39]. Quantitative deconvolution algorithms[40] can improve contrast for samples <20–30 μm thick or sparsely labeled specimens, provided that a properly sampled z-stack is acquired.

SD

SDs are generally optimized for live-cell imaging, using fast, sensitive cameras, and they excel at this application. Depending

on the camera, speed and sensitivity may come at the expense of resolution and/or field of view. Older instruments typically employed 512 × 512 pixel (i.e., 0.25 megapixel (MP)) electron multiplying charge-coupled device (EMCCD) cameras, with very high sensitivity but low resolution and a small field of view, but newer SDs may use higher-resolution, large-field-of-view sCMOS cameras. Most SDs are limited to imaging one color (single camera system) or at most two colors simultaneously (dual-camera system or single camera plus image splitter), such that multi-channel acquisition is rate limited by physical filter/mirror movements. Since the SD has many pinholes operating in parallel (Fig. 2b), images are collected much faster, but the scattered light prevalent in thicker samples may be imaged through the wrong pinhole (called 'pinhole cross-talk'), resulting in a loss of contrast when compared to CLSM[41]. Some newer SDs have multiple pinhole size and spacing options to counter this phenomenon.

CLSM

A CLSM provides superior resolution, depth penetration and contrast compared to a WF or an SD but is generally less sensitive and slower; thus, it is less well suited to live-cell imaging (Fig. 5a). CLSMs must scan a single laser beam across the specimen, generating the image one pixel at a time. Consequently, a CLSM is slower and requires higher laser power (lowering the score for sample viability). However, with the highly configurable hardware and software typical of modern CLSMs, the same instrument can be optimized for different experimental requirements. Figure 5b demonstrates how the key parameters for a CLSM, on the same instrument, can be optimized for either live-cell imaging (faster speed) or contrast (improved depth penetration and resolution). Resonant-scanning mirrors, which sweep the beam across the specimen 10 times faster than traditional galvanometer scanning mirrors, are closing the gap between CLSMs and SDs in terms of speed, but the consequent short dwell times require increased laser power or produce noisier images. CLSMs often have three or more detectors that can operate simultaneously, enabling rapid, multicolor live-cell imaging, particularly when combined with resonant scanning. New array detectors, such as the Airyscan (Zeiss), offer increased sensitivity and resolution simultaneously[42]. Higher sensitivity GaAsP (Olympus/Nikon/Zeiss) or hybrid (HyD; Leica) detectors more than double the efficiency of conventional photomultiplier tubes, allowing the laser power to be reduced. Using a larger pinhole also improves sensitivity and live-cell viability, while sacrificing z-resolution (see 'Setting up the microscope'). Indeed, the CLSM's flexibility to adapt to the experiment at hand makes it the workhorse of most microscopy core facilities[41].

Alternative optical sectioning methods

Other microscope techniques can offer a variety of advantages over confocal microscopes, depending on the experimental needs and biological questions. A multiphoton microscope uses a pulsed infrared laser to achieve greater depth penetration, and since the excitation volume of ~1 femtoliter is confined to a discrete location in x,y and z, it enables localized 3D photoactivation/photobleaching[43]. Total internal reflection fluorescence (TIRF) microscopy restricts excitation to ~100 nm adjacent to the coverslip surface, thus providing superior axial resolution and signal to background compared to confocal techniques, particularly for fluorophores in or near the plasma membrane[44]. For thick specimens such as whole zebrafish embryos or cleared tissues and organs[4], lightsheet microscopes offer advantages in both speed and low phototoxicity, though typically at the cost of resolution[45,46]. Super-resolution microscopes offer improved lateral resolutions of 100–140 nm (structured illumination microscopy), 25–50 nm (STimulated Emission Depletion (STED)), 20–40 nm (single molecule localization microscopy) or even 2–5 nm (MINFLUX)[47,48]. Axial resolutions can also be improved. The resolution enhancements typically come at the expense of speed, sample viability and depth penetration and are highly dependent on the sample itself, often requiring special fluorophores, smaller probes (e.g., nanobodies versus antibodies) and/or buffers.

Quantitative measurements of dynamics and interactions

Confocal microscopes (CLSMs in particular) are excellent platforms for a host of quantitative techniques for measuring molecular dynamics and interactions[49]. Fluorescence recovery after photobleaching (FRAP)[50] measures diffusion or binding of fluorescently tagged molecules by purposely photobleaching a sample region with high laser power, and subsequently recording the recovery of fluorescence as unbleached fluorophores exchange with the bleached ones. Photoactivation[51] or uncaging uses the opposite approach: laser illumination is used to selectively convert dark molecules to fluorescent ones, whose motion can then be observed. Fluorescence correlation spectroscopy (FCS)[52,53] and raster image correlation spectroscopy[54] measure concentrations, diffusion of fluorophores and other fluorophore behavior such as blinking (FCS only). These complementary techniques, which require rigorous acquisition and analysis[55], each have their own advantages and disadvantages for measuring cellular dynamics.

Measuring interactions between molecules is not a trivial task. Colocalization analysis (Box 1) does not confirm interactions between molecules, only that the two fluorescent tags are both located within a few hundred nanometers of each other (i.e., within the resolution limit of the microscope). Fluorescence resonance energy transfer (FRET)[56] experiments can be used to demonstrate that fluorescent probes on targets of interest are within 5–10 nm of one another, which typically confirms protein interaction. The major disadvantage of FRET experiments is that a negative result could arise simply from the fluorescent tags being further than 10 nm apart, even if the two tagged proteins are themselves interacting, or due to inappropriate orientation of the molecules relative to each other (i.e., dipole orientation)[57]. Alternatively, imaging co-dynamics of protein complexes is highly indicative of protein interactions. As an extension to FCS, dual-color dynamic imaging of two molecules of interest with fluorescence cross correlation spectroscopy[58,59] can be used to show co-dynamics. Finally, the proximity ligation assay has been developed to identify proteins/targets within ~40 nm of one another (suggestive of interaction) in fixed samples using antibody staining protocols[60].

Box 1 | The hazards of colocalization

Colocalization analysis can be a powerful tool for assessing the spatial relationship between two probes. There are several approaches[38,39], many of which have been implemented in open source software. Colocalization can indicate that two probes are generally near each other, but not that they interact. The accuracy of colocalization (i.e., just how close two molecules are) is limited by the resolution of the imaging system, which ranges from ~200 × 200 × 800 nm for a confocal down to tens of nanometers for some superresolution methods[47]. In the confocal microscope, colocalization analysis can therefore at best indicate that two proteins, each a few nanometers in diameter, are within 200–800 nm of each other. Moreover, the choice of labeling technique will also influence the distance between two fluorescent labels. If an indirect antibody labeling approach is used, the fluorochrome can be positioned up to 20 nm from its target epitope. Hence, while colocalization provides an initial hint as to whether proteins could be positioned close enough to interact, other imaging methods (FRET, fluorescence cross correlation spectroscopy or proximity ligation assay; see 'Quantitative measurements of dynamics and interactions') or biochemical means are required for verification. When measuring colocalization, keep in mind the following hazards that can produce false-positive and -negative results.

You see apparent colocalization where there should be none due to:
- Cross-reactivity between the two sets of primary and secondary antibodies;
- Binding of your primary antibodies to unexpected additional proteins with similar epitopes;
- Excitation cross-talk between the two fluorophores;
- Emission cross-talk/'bleed-through' between the two fluorophores, particularly problematic if the signal intensities of the two channels are wildly different;
- High background or autofluorescence in one or both channels;
- Use of hardening mountant so that the tissue is compressed along the z-axis, causing the signal from a fluorophore labeling one area of the sample to appear in the same 3D-voxel as the signal from a different fluorophore labeling another region above or beneath;
- Insufficient axial resolution to discriminate between cells overlaying each other due to the pinhole being opened too far;
- Low-NA objective lens leading to poor lateral and axial resolution;
- Spherical aberration caused by RI mismatch or use of the wrong coverslip thickness, leading to poor axial resolution;
- Insufficient sampling (pixel size too large);
- Inappropriate analysis such as:
  - failing to exclude background pixels from the analysis;
  - using a pixel-based intensity correlation algorithm in a sample with high background signal in both channels;
  - setting inappropriate thresholds for one or both channels;
  - using pixel-by-pixel colocalization analysis when object colocalization would be more appropriate.

True colocalization within a certain feature is not detected, due to:
- Variable abundance (due to endogenous protein levels or overexpression) of the two proteins of interest in the cell or variable localization to the structure of interest with one protein being expressed/localized at ≥10-fold higher concentration than the other;
- Poor labeling, often due to incomplete penetration of primary and/or secondary antibodies into the specimen;
- Variable brightness of the two dyes due to fluorescence quantum yield, numbers of antibodies/fluorophores per antibody binding each target, laser powers, emission filter settings and sensitivity of the detectors to the two different colors of fluorescence emission. Any of these contributions would cause a mismatch in brightness between the two channels, such that a simple overlay of the two appears visually almost identical to the single-labeled image;
- Poor SNRin one or both channels;
- Lateral or axial chromatic aberrations in the objective;
- Misaligned lasers or filters in the microscope;
- Inappropriate analysis such as:
  - setting inappropriate thresholds for one or both channels;
  - using pixel-by-pixel colocalization analysis when object colocalization would be more appropriate.

Planning your experiment

Pilot projects

Experimental design, data acquisition and data analysis may seem to be consecutive steps in the experimental pipeline, but in fact they form a continuous feedback loop, each one informing the others. Lessons learned in the 'final' step of data analysis can inform the overall design of an experiment, as well as the parameters used to acquire the data. A pilot project is an excellent way of starting this feedback loop in motion. It provides an opportunity to validate a quantitative imaging pipeline on a smaller scale before investing time, energy and resources in a full-scale experiment.

A good pilot project involves performing every step of the process all the way through to generation of a final output graph. Running through the entire process identifies issues that require fine-tuning. Live-cell imaging involves compromises between spatial resolution, temporal resolution, signal intensity and sample viability (the so-called 'tetrahedron of frustration'). Unanticipated limitations (e.g., poor cell viability or lower intensity than expected) may necessitate adjustment in cell preparation or experimental parameters. Small changes in image acquisition parameters often result in data that are far more readily analyzed and potentially meaningful. For example, a small reduction in spatial resolution could result in a critical improvement in signal intensity, allowing improved segmentation and quantification. A pilot project also presents opportunities to observe unexpected phenomena, thereby increasing the ways in which an experiment can be analyzed. For example, a change in localization of fluorescent vesicles might be accompanied by an unexpected change in fluorescence intensity, or vice versa. Preliminary measurements are often required in drug-treatment experiments to determine the time point at which maximum effect is obtained. A pilot project also provides an initial estimate of the strength of the predicted biological effect, which helps to estimate the number of samples that must be imaged to confidently measure the effect. For example, if, in the pilot study, there is only a subtle change of 25% between two conditions, then 100 images may be needed for each condition to measure the change with statistical confidence; however, if there is a twofold change, 30 images may suffice

(see 'Statistics'). Finally, a pilot study can be used to determine the brightest experimental condition, allowing you to set up the confocal microscope acquisition with appropriate intensities for the entire set of samples (see 'Configuring and optimizing fluorescence channels').

Removing bias

Bias can taint any experiment, including those that use confocal microscopy[61]. If slide #1 is expected to have brighter labeling than slide #2, your eyes might be drawn (either consciously or subconsciously) to capture brighter cells in slide #1. When reviewing images, you might think of reasons to throw away images that skew the average intensity in the 'wrong' direction based on the desired result. If microscopy experiments are to yield true and reproducible conclusions, ways of preventing human biases from affecting image capture and analyses must be found.

In clinical research, the gold standard is to conduct a randomized, double-blind, placebo-controlled study[62]. Both researcher and subject are blind to whether the subject is receiving the treatment or the placebo; blinding ensures that subjective measurements, such as improvement in patient-reported pain, are not influenced by expected or desired outcomes. Most confocal microscopy users, however, will prepare, image and analyze their own slides, which often includes subjective choices such as which fields of view to capture or what threshold to set for counting positively labeled cells. Consider asking a colleague to label the slides so that you are blinded to control and experimental conditions until image acquisition and analysis are complete.

When imaging tissue sections, remove the field-of-view selection bias by imaging and analyzing entire structures or even the entire tissue. Confocal microscopes equipped with motorized stages can be set up for tiling and stitching large regions in 2D or 3D. Since 3D z-stacks can be time consuming, consider limiting the acquisition to 20× or even lower, if that resolution is sufficient. To quantify labeling in very large samples such as whole organs, tissue clearing[4] combined with light-sheet microscopy[45,46] may be a better choice. However, be prepared for extremely large datasets: a single whole-organ light-sheet dataset can be as big as 1 TB, requiring special computer infrastructure for handling, viewing, rendering and quantifying the signal. Alternatively, physically slicing thin tissue sections (5–15 μm) enables them to be scanned on increasingly common whole-slide fluorescence scanners. Regardless of whether it was scanned on a widefield slide scanner or tiled on a confocal microscope, whole-slide analysis software (e.g., Halo (Indica Labs), StrataQuest (Tissuegnostics), VisioPharm, Harmony (PerkinElmer) or the new freeware QuPath[63]) can quite easily quantify nuclear, cytoplasmic and membrane labeling across an entire tissue (among other features). Traditionally, whole-slide analysis was complicated by the fact that recognizing structures in the tissue still had to be done by a qualified pathologist, but the machine learning–based pattern-recognition classifiers available in each of these software packages make it easier to separate tissue types (e.g. tumor versus stroma) by training the algorithm with example regions[64,65].

In the field of neuroscience, stereology rose to prominence from 1970 to 2000 as an unbiased and accurate way of estimating geometrical features (e.g., number, length, volume, etc.) in 3D structures from 2D brain slices[66]. Stereology, which can be performed on both widefield and confocal microscopes, adds a software component that provides random, systematic sampling according to rigorous statistical principles. However, stereology will only be successful if unbiased sampling is achieved, which starts with the very first decision on how to section the tissue. As whole-slide scanning and 3D imaging and analysis techniques have developed and can now quantify the entire sample in 2D or even 3D, the use of stereology has declined[67]. While stereology may not be necessary for most experiments, confocal microscope users must still put sufficient thought into rigorous specimen sampling.

Setting up the microscope

With so many components to configure, setting up a confocal microscope for quantitative image acquisition can be a daunting task. The step-by-step guide in this section provides a workflow for the most important aspects of configuring the microscope.

Stage inserts

It can be surprisingly difficult to ensure that samples are mounted flat and stable on the microscope. A variety of interchangeable stage inserts are usually available; check that one is properly installed and leveled. Mounting the sample itself into the stage insert, to be held firmly and presented exactly perpendicular to the optical axis, can also be challenging. If the sample is mounted correctly, it will remain in focus while scanning across the coverslip. For imaging slides on an inverted microscope, ensure that only the edge of the glass slide is resting on the insert (not the coverslip or label). If you are using coverglass chambers together with high-NA objective lenses, keep the center of the objective lens away from the edge of the chamber to avoid the lens hitting the stage insert; unfortunately, it is often not possible to image right to the edge of these chambers.

Selecting an objective lens

One of the most critical decisions is choosing the ideal objective lens for the specific experiment (Fig. 6 and Table 1). The most significant factor in determining both sensitivity and resolution is not the magnification but the NA of the objective, which is prominently indicated next to the magnification on the lens (e.g., 20×/0.8 NA). The NA is defined by the half-angle of the cone of light that is focused or collected by the objective (θ), and the index of refraction of the mounting medium (n):

$$NA = n \cdot sin\theta \quad (2)$$

From the resolution equation (Eq. 1), it is clear that doubling the NA, even at the same magnification, results in twice the resolution (i.e., features that are twice as small can be resolved). Perhaps even more importantly, when the NA is doubled, the amount of light collected from the sample is four times higher: high-NA objective lenses are crucial for capturing fluorescence

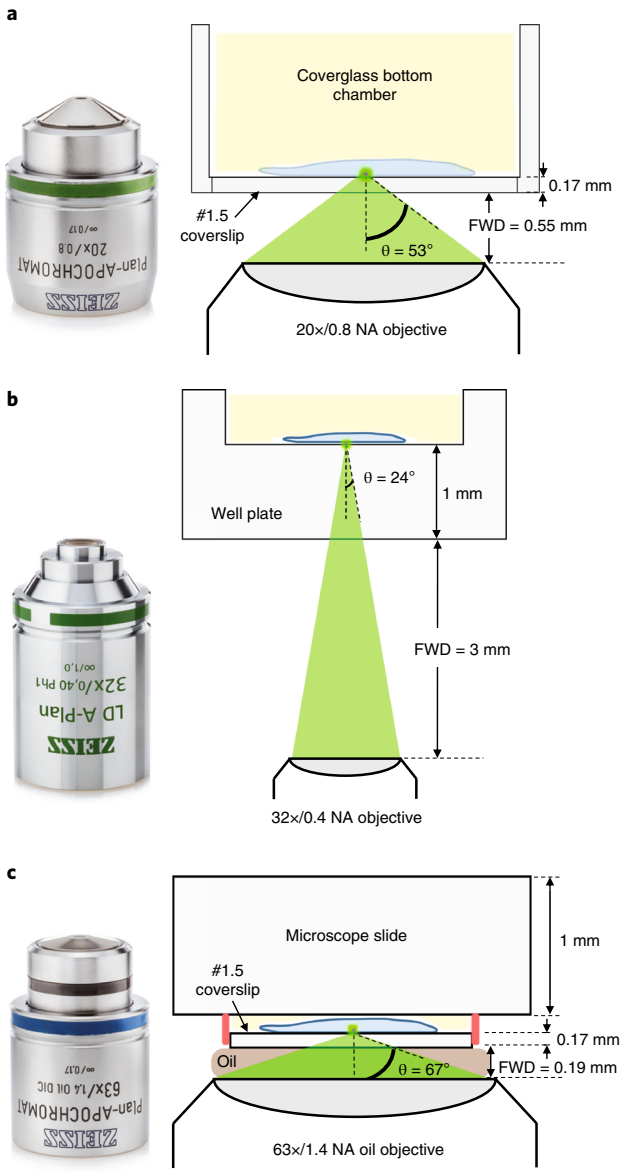

Fig. 6 | Objective lens comparisons. a, 20×/0.8 NA Plan-Apochromat objective lens corrected for a standard #1.5 (0.17-mm) thickness coverslip. The high NA (resulting in a steep focusing/collection angle of $\theta = 53°$) provides high resolution and sensitivity but leaves a full WD (FWD) of just 0.55 mm. **b**, 32×/0.4 NA A-Plan objective optimized for a 1-mm plastic-bottom dish. The FWD is a generous 3 mm, but this comes with a reduced resolution (half) and sensitivity (one-quarter) compared to the 20×/0.8 NA objective. The built-in phase ring makes it convenient for finding unlabeled cultured cells but further blocks fluorescence emission. **c**, 63×/1.4 NA oil immersion Plan-Apochromat objective corrected for a #1.5 coverslip. Oil immersion boosts the NA to provide nearly double the resolution and four times the sensitivity of the 20×/0.8 NA dry objective, but the short FWD limits imaging to near the coverslip.

efficiently. However, be aware that the laser is focused to a smaller spot, so the irradiance (laser power density) during excitation is also higher, which has consequences for photobleaching and sample viability. Since the NA of an objective depends on the refractive index of the immersion medium, an oil immersion lens ($n_{oil} = 1.518$) can have a higher NA than a water lens ($n_{water} = 1.33$), while a dry lens ($n_{air} = 1.0$) will have even lower NA. Should oil immersion lenses always be used for fluorescence microscopy? No. First, the high NA of oil immersion lenses comes with the trade-off of a shorter WD (i.e., the distance from the objective front lens to the closest coverslip surface when the sample is in focus), typically <200 µm. The short WD makes it compatible only with imaging through a coverslip (Fig. 6c) and limits the depth of imaging into the sample. Tissue culture microscopes will instead be equipped with lower-NA, longer-WD dry objectives (Fig. 6b) that are adequate for seeing cells through thick tissue culture plates or flasks, but with lower resolution and sensitivity. Special long WD water or glycerol immersion objectives are more expensive but maintain reasonably high NA. Second, mismatch between the RI of the immersion medium and that of the sample can cause spherical aberration artifacts, and their severity increases deeper into the sample. Thus, when imaging a thick biological specimen, with an RI that is very different from standard immersion oils, or a cell monolayer in aqueous medium, the advantages of using a water, glycerol or silicone oil immersion lens to attain a better RI match may outweigh the disadvantage of slightly lower NA. Compare different objectives to see which works best. If the objective has a correction collar, it must be set at the position for the corresponding immersion medium, coverslip thickness and/or temperature, or better still, adjusted while imaging (assessing by maximal image sharpness and brightness) to compensate for the thickness variation of even a standard #1.5 coverslip. Third, consider what resolution is needed for the experiment: a 20×/0.8 NA dry objective (Fig. 6a) gives a field of view as high as 0.5 × 0.5 mm (nearly 10 times that of a 63× objective lens), while still providing a resolution of 400 nm, which is more than adequate for quantifying nuclear intensities, for example. This high-NA dry objective may also be an excellent choice for long-term, medium-resolution, multi-location timelapse imaging of live cells. Unlike most camera-based microscopes (including SDs), the optics within a CLSM allow for true optical zoom during acquisition (rather than digital zoom on the acquired image), so that there is no resolution advantage, for example, in using a 100×/1.4 NA objective lens over a 63×/1.4 NA objective coupled with 1.6× zoom. The lower magnification lens offers a larger field of view and brighter image (though the increased brightness is the result of more laser illumination reaching the specimen (Supplementary Fig. 1)).

Once the objective lens is selected, ensure that it is clean (dried oil left on the lens by a previous user is a common problem). If required, clean it with specialized lens tissue (avoid waxy 'lens paper') or cotton-tipped applicators and an appropriate lens-cleaning fluid. The delicate front lens of an objective lens is often concave, so care and repetition are required to clean them properly. If necessary, use a magnifying glass to closely inspect the front (and sometimes rear) lens surfaces.

Working with live cells

For confocal imaging of live cells[23], maintaining an appropriate physiological environment (temperature, pH and humidity) is essential. Either stage-top incubators or large microscope enclosures can be used for this. When using immersion lenses

Table 1 | Some common objective lenses, key specifications and applications

Magnification/NA	Immersion	FWD	Example application
20×/0.8 NA	Air ($n = 1.0$)	0.55 mm	Moderate resolution confocal
20×/1.0 NA	Water ($n = 1.3$)	2.1 mm	Intravital confocal/multi-photon
32×/0.4 NA	Air ($n = 1.0$)	3.1 mm	Widefield cell culture
40×/0.95 NA (correction collar)	Air ($n = 1.0$)	0.25 mm	High-resolution slide scanning
63×/1.2 NA (correction collar)	Water ($n = 1.3$)	0.28 mm	Live-cell confocal (>10-μm depth)
63×/1.4 NA	Oil ($n = 1.518$)	0.19 mm	Fixed-cell confocal; live cell <10 μm from the coverslip

There is much more than just the magnification to consider when choosing an objective lens. The NA determines the resolution and sensitivity of the lens but also affects the FWD.

with stage-top incubators, a separate objective heater must be employed to prevent the objective from acting as a heat sink. Humidification of environmental control chambers is often inadequate: to avoid changes in osmolarity due to evaporation, place wet tissues in the chamber, or fill empty wells or space between wells of a multi-well plate with water. Since focus drift is endemic on microscope stands, use hardware autofocus devices (such as Zeiss's Definite Focus, Nikon's Perfect Focus, Leica's Adaptive Focus Control or Olympus's Z-Drift Compensator to ensure that focus remains stable during timelapse experiments.

Most cells or tissues are never exposed to light in their natural physiological environment, making them particularly sensitive to fluorescence illumination. One side effect of photobleaching is the production of highly reactive and damaging oxygen radicals that cause phototoxicity. Consider whether the live imaging question requires confocal microscopy at all: many experiments such as cell tracking, proliferation or wound healing[68] can be addressed using transmitted-light techniques (e.g., phase contrast or DIC; Box 2). Shorter wavelength light is considerably more phototoxic to cells than longer wavelengths, so avoid blue-emitting dyes for live-cell work when possible.

Finding the cells

Most confocal users (present authors included) use binoculars to search the slide for representative cells or the most meaningful features in the tissue. Using transmitted light (such as DIC) to find the areas of interest will reduce photodamage to the sample, but many users find it easier to use widefield fluorescence visualization for its higher contrast or its ability to rapidly locate specific fluorescently labeled features, cells with reasonable protein expression levels or dual-expressing cells. However, the sample is prone to rapid photobleaching during this preliminary observation! Figure 7 shows a field of view that was observed with a typical metal halide lamp (X-Cite 120Q, Excelitas) for just 60 s on the maximum intensity setting while centering and focusing on the cells. Even the relatively stable fluorophore Alexa Fluor 488, mounted with Prolong Gold antifade mounting medium, bleached by 50% in just 3 s, and by 75% in 10 s. The time spent on each field of view before even beginning to collect confocal images can destroy a substantial amount of fluorophore and has a potentially significant influence on the eventual measured intensities.

To minimize photobleaching:

- Adjust the light source to its lowest setting, usually ~10% (use neutral-density filters to go even lower for live cells), and allow your eyes to adjust to the dimmer setting (turn down/off the room lights). This single act will reduce the photobleaching dramatically.
- Close the fluorescence shutter the second you finish observation.
- For very sensitive experiments, use transmitted-light contrast techniques or the red fluorescence channel to focus and find the cells.
- Establish the acquisition settings on a test region, and then acquire experimental data from an unexposed area of the sample.

Configuring and optimizing fluorescence channels

As outlined in the sections on sample labeling, it is critical to understand the excitation and emission profiles of the fluorophores you are using. The excitation and emission spectra for a typical combination of four fluorophores is shown in Fig. 8a. On a CLSM, setting up fluorescence channels for multiple fluorophores from scratch can be bewildering. Since many of the spectra overlap, what is the best way to collect each fluorophore's emission as efficiently as possible, while avoiding excitation and emission cross-talk (also called 'bleed-through') from the other fluorophores? Fortunately, most CLSMs have a software wizard to help get you started: simply select the fluorophores from a list, and choose one of the various multichannel strategies (Fig. 8b–d). Many CLSMs have three or more detectors and allow illumination with multiple lasers simultaneously. However, simultaneous excitation should generally be avoided to minimize cross-talk (Fig. 8b). The nuclear stain DAPI has a particularly broad emission that extends all the way to 600 nm (red), and will bleed through into the green and red channels in simultaneous scan mode (Fig. 8e–g). Simultaneous scanning should be used only when speed is of the essence in the fastest of live-cell imaging experiments (post-acquisition cross-talk corrections should then be applied if necessary). A second strategy looks tempting (Fig. 8c), here imaging two colors with low overlap (DAPI and AF568) simultaneously and the fluorophore between them (AF488) on a separate pass of the lasers. Unfortunately, this schematic offered by the wizard can be misleading because it assumes that all the fluorophores have equal intensities: if DAPI is much brighter than AF568, there will still be substantial bleed-through of DAPI emission

Box 2 | DIC complements fluorescence

With confocal fluorescence microscopy, sometimes the fluorescence labeling is punctate or filamentous, such as the Keratin5-GFP labeling in keratinocytes shown on the left panel in the figure below. It may be important to get an overall picture of the cell, for example, to measure cell boundaries, assess cell state or confirm cytokinesis. Rather than labeling the cell with additional fluorophores, which may contribute to phototoxicity or otherwise perturb the cell's normal functions, consider adding a transmitted-light image. DIC can produce sharp images of cell and organelle boundaries as shown on the right, complementing the fluorescence image (see figure below and Supplementary Video 1).

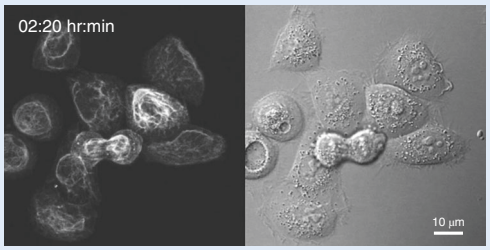

Unlike phase contrast, in which a dark phase ring built inside the objective to produce contrast unfortunately blocks precious fluorescence photons, DIC objectives have no effect on fluorescence intensity. However, the analyzer, when inserted under the objective, reduces intensity, and the DIC prism skews the PSF of the microscope, reducing the resolution and degrading fine image details[97]. It is ideal if the microscope stand is equipped with a motorized analyzer and prism that can be automatically inserted for DIC imaging and retracted for fluorescence imaging. Since DIC uses polarized light, it cannot be used with plastic dishes, which destroy the polarization. If the microscope is not equipped for DIC, or plastic dishes must be used, try closing down the condenser diaphragm to generate some contrast. The resulting 'dirty brightfield' image is so called because it projects blemishes (dust, condensation, etc.) into the image plane that are not visible with proper Koehler-illuminated DIC, but the added contrast may suffice for some experiments (e.g., if cell shape or stage of the cell cycle must be determined).

Four components are needed to achieve DIC (two polarizers and two prisms). To add in these DIC elements:

- Adjust the transmitted-lightpath for Koehler illumination:
  - focus on the specimen;
  - close down the field diaphragm;
  - adjust the condenser focus to bring the edge of the field diaphragm into focus;
  - center the field diaphragm in the field of view;
  - open the field diaphragm back up to just outside the field of view;
  - remove one ocular, and adjust the condenser (aperture) diaphragm to ~2/3 of the full field of view seen with the ocular removed.
- Insert two polarizers for viewing DIC in the binocular. One polarizer is subsequently removed for confocal acquisition since the lasers are already polarized.
- Adjust the second polarizer (sometimes called the 'analyzer') to make the field of view as dark as possible.
- Insert two prisms—one below the objective and one in the condenser turret. Adjust the skew on the objective prism to produce the desired contrast.

into the AF568 channel. The safest (though slowest) strategy is to image each channel sequentially (Fig. 8d), with one laser and the corresponding detector turned on at a time. It is often preferable to switch channels line by line rather than frame by frame to avoid temporal delays between channels. To maximize speed in multicolor imaging, try to configure the channels so that no mechanical components are moved between channels. The wizard configurations are only a starting point and are rarely optimal. For example, some CLSMs have fixed emission filters, but the confocal pictured here has adjustable filter 'gates' that could be further narrowed or broadened to improve specificity or sensitivity, respectively. To ensure reproducibility between experimental replicates, configuration files can be saved and loaded during subsequent sessions, or settings can be applied from a saved image. For an SD equipped with one camera and fixed filters, the configuration is much more straightforward: simply choose the three fluorescence channels, and there is probably a single corresponding configuration.

Sometimes cross-talk is unavoidable, for example, when using CFP and YFP for a FRET study, or when using more than four fluorophores at once. Spectral unmixing[69] allows the separation of several fluorophores with overlapping spectra after acquisition. Caution is required with this approach. Good results will require single-labeled controls for each fluorophore to measure accurate reference spectra, and it is critical to balance the labeling intensity for each fluorophore and ensure that the unmixing algorithms result in signal separation that is valid and artifact free.

Image the brightest sample first, such as a positive control. Optimize the intensity of each fluorophore, turning on just one channel at a time to prevent photobleaching of the others. Start with a low laser power, ~1–5% of the maximum, to minimize photobleaching and then increase from there as necessary. On a CLSM, begin by setting the pinhole diameter to 1 Airy Unit (AU), which is typically a good balance between optical section thickness and signal-to-noise ratio (SNR)[70]. The pinholes on an SD are fixed in size, but several size and spacing options may be available. Start a live preview, and then adjust the detector sensitivity (sometimes called 'gain' or 'high voltage' on CLSMs) or camera exposure time (SD) until an image is observed. Adjust the focus to select the brightest focal plane. If the fluorescence is unexpectedly weak or the image is blurry, refer to the troubleshooting steps in Box 3. If the image is too noisy, reduce the detector gain (CLSM), slow down the scan speed so that the pixel dwell time is ≥1–3 µs and/or use line or frame averaging (typically two to four averages). For an SD, adjust the camera settings such as increased exposure time, pixel binning or reduced readout speed. For fast processes, it may be

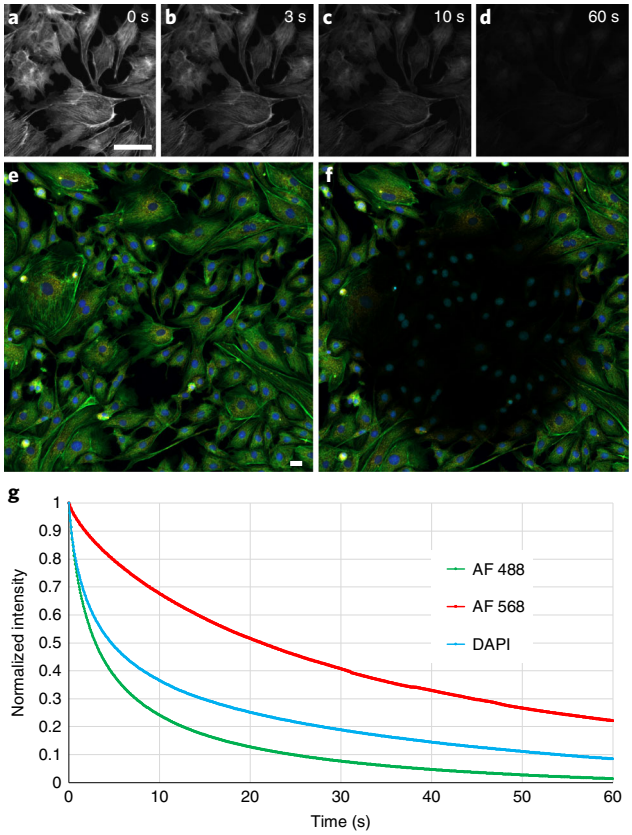

Fig. 7 | The effects of photobleaching during widefield observation. When preparing for confocal imaging, finding and focusing on your sample using the binocular may result in a significant (but unknown) amount of photobleaching. BPAE cells (Fluocells Prepared Slide #1, Thermo Fisher Scientific) labeled with DAPI (blue), AF488 phalloidin (green), and MitoTracker Red (red) were sequentially illuminated with an X-Cite 120 widefield fluorescence lamp through a 63×/1.4 NA oil immersion objective for 60 s (from red to green to blue channel). **a**–**d**, AF488 image after 0, 3, 10 and 60 s, respectively: in just 3 s, the AF488 intensity is half of its initial intensity, and by 60 s, the fluorescence is completely gone. **e** and **f**, Switching to the 20×/0.8 NA dry objective before and after photobleaching (lamp set to 12% power) shows the dramatic decrease in fluorescence in all channels from just 60 s of widefield observation. DAPI has bleached, but photoconversion of DAPI is apparent in the green channel after strong UV illumination. **g**, Normalized intensity of the three fluorophores during 60-s widefield observation at full lamp power. Scale bars = 50 µm.

necessary to increase the laser power while monitoring photobleaching and/or phototoxicity. To optimize the intensity levels, confocal microscopes have a special lookup table (color map) to reveal areas on the image with pixels that are too bright ('saturated') and pixels that are zero intensity (Fig. 8h–k). If any type of quantification is to be performed, it is imperative to avoid any 'clipping' of either the brightest or dimmest pixels. Acquire the raw data across the entire intensity range; afterwards, digital contrast adjustments or background intensity subtraction may be used to reveal the features of interest, applying the same adjustments to all images to be compared as described in Analyzing and presenting quantitative images. To maintain the same settings for all specimens, the settings chosen must encompass the full range of intensities across them all, so it is critical to begin with the brightest sample to avoid saturation throughout. Using a higher bit-depth setting (16-bit, rather than 8-bit) gives a greater number of gray levels between black and white, which may allow the capture of subtle intensity differences in both the brighter and weaker features of a specimen. If it is impossible to image a bright and a weak sample with the same settings, adjust the laser power (CLSM) or exposure time (SD), since these usually vary linearly, and acquire a second set of corresponding images. Take note of the two laser power settings, or more rigorously measure them with a power meter through the objective lens, so that the difference can be accounted for during analysis.

Optimizing spatiotemporal parameters

Having adjusted the intensity for each fluorescence channel, next, establish the set of parameters that affect the size and shape of the image and the speed of acquisition. Note that some of these settings affect the fluorescence intensities somewhat, so channel re-optimization may be required. The default zoom for a CLSM (zoom 1) will set the confocal to scan a square area roughly two-thirds of the way to the edge of the binocular field of view. The default image size of 512 × 512 pixels (0.25 MP) is generally insufficient to preserve the details of the sample, resulting in a pixelated appearance and making it difficult to analyze or generate high-quality figures for publication. Instead, use at least 1024 × 1024 pixels (1 MP), and/or zoom in to a smaller region of interest. For maximum image resolution, the pixel size should be two to three times smaller than the optical resolution of the objective lens as calculated by Eq. 1—a condition called 'Nyquist sampling'. Some CLSM software programs have an 'optimal' button that, given the current objective lens and zoom, calculates the number of pixels you need to achieve Nyquist sampling. Since a CLSM scans one pixel at a time, if the maximum field of view is selected (e.g., zoom 0.7) with Nyquist sampling (say, 4096 × 4096 pixels), it may take several minutes to acquire a single (2D) confocal image. Some compromise may therefore be required to balance the quality of the image with the acquisition time: for example, if the smallest structure that must be resolved is larger than the objective's maximum resolution, the Nyquist calculation may be applied to the structure size instead. The scan speed is also adjustable: aim for a pixel dwell time (reported in the software) of ~1 µs/pixel to minimize noise in the images. While SDs lack the zoom flexibility of CLSMs, there may be options for reading out subregions or binning of a CCD chip, or possibly switching between cameras with different pixel size or field of view.

Having optimized a single XY (lateral) image, apply the same principle of sampling to the Z (focus) dimension. The optical sectioning thickness depends on the NA of the objective and the size of the pinhole(s). On a CLSM, the software should report the slice thickness as the pinhole size is changed, and then automatically calculate the optimal z-interval based on the Nyquist sampling theory of two to three overlapping z-steps per optical slice thickness. SDs may not indicate the required z-step for Nyquist sampling, requiring prior knowledge of the maximum achievable z-resolution with a given objective lens. As a rule of thumb, the slice thickness is about three times the Nyquist pixel size in x,y and will be ~1 µm for a 63×/1.4 NA oil immersion objective on an SD.

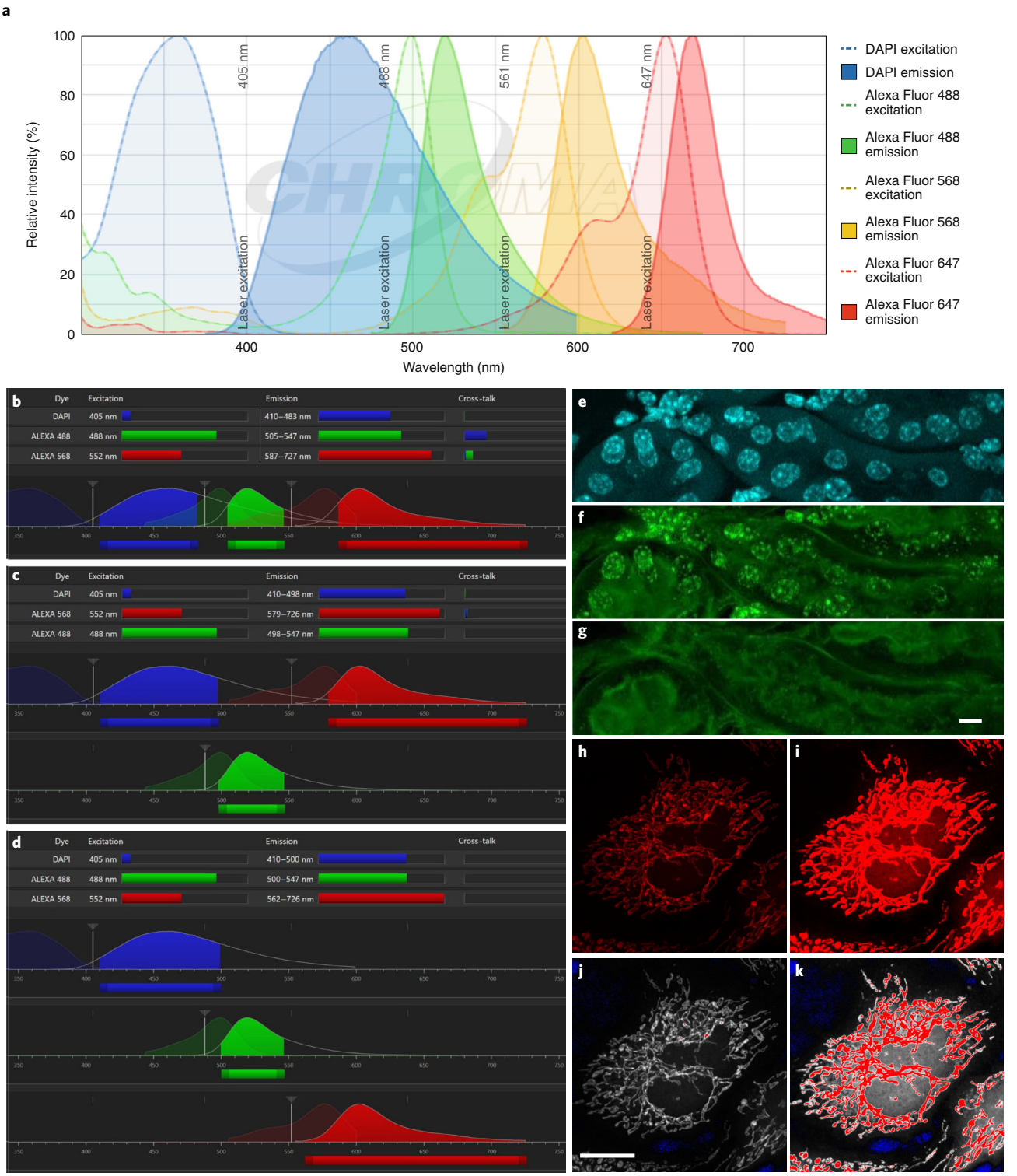

Fig. 8 | Configuring confocal detection channels. a, A screenshot from Chroma Technology's Spectra Viewer shows excitation and emission spectra from four fluorophores (DAPI, AF 488, AF 568 and AF 647). With sequential acquisition, these (or equivalent) fluorophores can be acquired without any cross-talk. Credit: Chroma Technology. **b**–**d**, Screenshots from one of the CLSM configuration wizards, showing simultaneous (**b**), semi-sequential (**c**) and fully sequential (**d**) strategies for capturing three fluorescence channels. To speed up acquisition, the semi-sequential approach is often recommended by the vendors, but if DAPI is significantly stronger than AF568 in this example, there will be considerable bleed-through of the DAPI signal into the AF568 channel. **e**, Pure DAPI channel from a kidney tissue showing labeled nuclei. **f**, Nuclear bleed-through into the green AF488 channel when these two channels are imaged simultaneously. **g**, The pure AF488 is seen when the DAPI laser is switched off; the nuclear signal is no longer visible. **h** and **j**, MitoTracker Red staining imaged using correctly adjusted acquisition settings and displayed in red pseudocolor (**h**) and grayscale with saturation Look-Up Table (LUT; **j**). **i** and **k**, MitoTracker Red staining imaged with higher laser power or gain and shown in red pseudocolor (**i**) and grayscale with the saturation LUT clearly indicating saturated pixels in red (**k**). Scale bars = 10 μm.

Box 3 | Troubleshooting unexpectedly weak fluorescence or blurry images

Having prepared a fluorescent specimen and mounted it on the confocal microscope, how should you proceed if your image is unexpectedly weak or blurry? Is the problem with the microscope, the specimen or both? Pay close attention to the microscope lightpath and optical properties of the sample, including mounting medium, immersion medium and coverslip, and try following these steps:

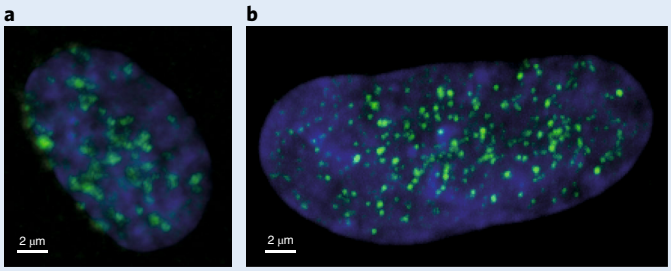

Is it the microscope?

1 If there is no signal at all, in either the binocular or in confocal mode:
- Are all of the hardware components (main switch/laser, including key, microscope stand) turned on?
- Trace the lightpath from the light source to the sample, and from the sample to the eyepieces or detector, checking each component.
- Can you see whether laser light is emitted from the objective lens?
- Is the software configured appropriately (sufficient laser power, sufficient gain/high voltage)?
- Have you tried switching it off and on again? Restart the microscope software and/or the entire system in case a component has not initialized properly.

2 If the sample appears weak and/or blurry in the binocular:
- Is the fluorescence lamp on and dialed to an appropriate power level? Keep the light intensity low to avoid photobleaching, dim the room lights and allow your eyes to adjust.
- Is the objective lens rotated properly into position?
- Is a polarizer (for DIC) inserted into the beam path, between the objective and the detector? If so, remove it; this component is not needed to perform confocal DIC.
- Is the objective lens clean? Follow your vendor or facility instructions for cleaning the objective, usually with lens-cleaning solution and lens tissues. Dried oil may take two or three tries to remove. Different solvents may be required (e.g., water for media salts), but always check that they are compatible.
- Could the objective be damaged (oil inside, scratched)? Take it out (or ask facility staff to have a look) and check it under a stereo microscope; if damage is suspected, acquire PSFs using beads/test samples.
- If your objective has a spring-loaded front lens, it could become stuck in the compressed position. It is also common to accidentally compress the lens elements while trying to focus near the edge of the stage adapter. This will bring the sample into focus, but with severe aberrations.
- Some specialized objective lenses have a correction collar that adjusts for the thickness of your coverslip or the RI of your mounting medium. Make sure this is set appropriately.
- Are you using the correct immersion medium for the objective?
- How does the sample look with a different objective or on a different microscope?

3 If the intensity appears normal in the binocular, but confocal images are weaker than expected:
- Adjust the focus up and down during a 'live' confocal scan—thanks to the pinhole, the tolerance is much tighter compared to widefield.
- Is the correct configuration setting (filters, beamsplitters, etc.) in place for the respective laser wavelengths and detector channels? Try re-loading settings from a previously saved 'good' image.
- Are the laser power and detector gain set to reasonable levels?
- Is the laser weak? Has it warmed up fully? Is it getting old (dying)?
- Do you get a similar intensity of signal if you send the emission to a different detector?
- Use a power meter to measure laser power through the 10× objective and compare with previous measurements.

Is it your specimen?

1 Basic checks:
- Have you used a #1.5 coverslip? Most confocal microscopes are equipped with objective lenses that require a #1.5 (170-μm-thick) coverslip (this is indicated on the lens). Ensure that there is only a single coverslip present (sometimes a stack of two or more may have accidentally been used).
- Replace your sample with one that you have imaged before and know to be good, or use a test slide such as a Convallaria section, H&E slide (green or red emission channels only) or Molecular Probes Prepared Slide #1 or #3. Can you get a 'good' image with the test slide? Compare the intensity and quality of a new test image to one that was previously captured on this microscope (reuse the same settings if possible).
- How deep are you imaging? Is your focal plane of interest within the WD of your objective? If you have fixed cells and you use a high-NA water objective (e.g., 63×/1.2 NA water), or if you have live cells and you use an oil objective (e.g., 63×/1.4 NA oil), the RI mismatch produces aberrations. The effect is not normally noticeable until you focus >10 μm into the sample: if you image thin cells grown right on the coverslip, this will not be a problem.

2 Has your label worked?
- If you have imaged a similar sample successfully before, did you change anything in the sample preparation (e.g., fixation, coverslip thickness, new/old batch of antibody, mounting medium)?
- If you are doing antibody staining, did your staining procedure work? Positive controls are key. If not, compare different primary antibodies against the same protein; also compare different secondary antibodies.
- Did your antibodies penetrate throughout the whole thickness of the specimen, or do you need to test different fixation/permeabilization combinations?
- Is your mountant/antifade compatible with the fluorescent probes used (Fig. 4)?
- For live cells, did your transfection work? Cell sorting may detect faint signals (the sum of fluorescence from the entire cell) that are not sufficient for confocal imaging.
- FP signals may quench when fixed; try imaging a live sample, or consider using antibody labeling against the FP with a bright, photostable fluorophore.

Box 3 | Troubleshooting unexpectedly weak fluorescence or blurry images (Continued)

3 Has the sample been damaged or degraded?
- Have you already imaged it extensively, so that it may be photobleached?
- Is this an old sample? How was it stored (in the dark, temperature)? Over time, some fluorophores diffuse from the structures they were labeling.
- Tissues may be damaged if the coverslip has slipped, particularly if non-hardening mounting medium is used without sealing the slide. Tissues may also degrade if they have been stored for a long time in the freezer.

The CLSM is adaptable—recall Fig. 5b, where it was shown that the same CLSM can be optimized for either fixed or live-cell applications. When contrast is the priority, keep the pinhole at the theoretical optimum of 1 AU and consider slowing down the scan speed, and averaging two to four images while reducing the detector gain. If the fluorescent dye is stable or only one or a few images need to be collected, then consider increasing the laser power. The radar plot (Fig. 5b, red curve) shows that this combination benefits depth penetration and resolution, but particularly compromises the speed of acquisition (which can climb to several minutes for a small z-stack) as well as sample viability. When optimizing for live-cell imaging (Fig. 5b, green curve), suggested settings for optimal speed and lower phototoxicity include simultaneous instead of sequential channel acquisition, the use of higher sensitivity GaAsP or hybrid detectors, lower laser powers, faster scan speeds (with regular galvanometer or resonant scanners), a pinhole diameter >1 AU and increased detector gain. These parameters sacrifice contrast, depth penetration and resolution but make CLSMs compatible with live-cell imaging.

Troubleshooting instrumentation issues

With a new understanding of how to prepare optimal samples and set up the confocal microscope with appropriate settings to avoid photobleaching, saturation or cross-talk between channels, you feel ready to acquire quantitative data. You plan to image all of your slides in one 3-h session, using the same settings, and have taken steps to ensure that you select fields of view in an unbiased manner. What could possibly go wrong? Despite carefully executing the confocal imaging experiment, a quagmire of unexpected instrumentation issues may still prevent quantitative results. Be aware of the following problems as you use your confocal microscope.

Problem number 1: non-uniform illumination

Confocal microscope manufacturers try to configure and align the microscope with uniform illumination intensity across the field of view, but the lack of consistent design specifications and properties of the optical components and microscope design lead to variability. Figure 9a–c shows a particularly bad example on a CLSM from a 20×/1.0 NA intravital imaging objective, which has an unusually wide field of view, given its high NA and long WD (1.9 mm). At a zoom of 1, the intensity varies by 40% between the center of the image and the corners, and a massive 60% using the minimum scan zoom of 0.7×. This uneven illumination would lead to a 60% difference in the intensity of the same cell depending on where it was positioned in the field of view, adding considerable (and systematic) error to any intensity measurements. It also makes it difficult to set a simple intensity threshold for selecting positively labeled cells. Most CLSMs have ≥10% variation in their illumination (corner to center) at the lowest zoom, but at higher zoom (usually ≥1.5), the problem is less pronounced: for better intensity uniformity, users should consider zooming in and using tiling and stitching to achieve the desired field-of-view size. For SDs, traditional illuminators result in 20–60% variation across the field of view, though newer illuminator technology based on multimode fibers such as the Borealis (Andor) may reduce the variation to <10%[71]. For instruments with poor uniformity, users can image a uniform fluorescence sample such as a thick fluorescent plastic slide (Chroma, https://www.chroma.com/products/diagnostic-slides) or saturated dye solution[72] and apply a software correction called 'flat-field' or shading correction (note that the thick plastic slides do not work well for SDs, as there is significant pinhole cross-talk). However, since the illumination profile changes over time, they need to be re-measured regularly, which is often not practical. It would be helpful if the imaging community (both users and manufacturers together) would adopt a standard requiring 90% illumination uniformity at zoom 1, measured according to the recently created International Organization for Standardization (ISO) standard for CLSMs[73].

Problem number 2: focus drift

Many confocal microscope stands experience significant focus drift over time. This is revealed by an increasingly blurry image on a WF microscope, but on a confocal microscope, the rejection of out-of-focus fluorescence leads to a change in intensity as well as different features appearing in the image. Figure 9d shows how the focus on a new CLSM can take several hours to stabilize. This behavior might be anticipated when turning on an environmental chamber, since small changes in temperature expand the metal microscope stand, but not for this dataset recorded at a stable room temperature using a fixed slide. Our tests of six microscope stands by four different manufacturers revealed varying degrees of focus drift for all, with most stands requiring 2–3 h to stabilize (Supplementary Fig. 2). For live-cell imaging, the drift can be corrected by hardware autofocus devices as discussed above ('Setting up the microscope'). However, these devices are dependent upon a significant RI mismatch between sample and immersion medium and are therefore often incompatible when imaging fixed cells, in hardened mountant, with oil immersion lenses. Moreover, they may be insufficient to counteract drift over the particularly long image acquisition times required for tiling or superresolution. Consider turning the instrument on ≥1–2 h before starting imaging, or even leaving the confocal microscopes powered on 24/7. Not only will this enable the focus drive to warm up, but also other optical components (motorized filter wheels, pinholes, etc.) that may affect the image in less noticeable ways. We encourage the manufacturers to adopt a standard whereby the microscope should stabilize to <1-μm

focus drift/h within the first hour after initialization, and to develop routine tests to identify and replace or repair faulty focus drives when necessary.

Problem number 3: laser instability and power variation

Laser instability is perhaps the most insidious and common (though largely unappreciated) instrumentation issue for CLSMs. Figure 9e shows how one model of femtosecond laser (used for multiphoton microscopy) performed during the first hour of operation after being keyed on from standby mode. The laser started emitting after ~5 min, but there was a dramatic change in intensity when the laser cavity automatically re-optimized 30 min after start-up. Even worse, over the next hour, if the laser was tuned to a new wavelength, it again automatically re-optimized, causing the power to change by a further 15%; however, if the wavelength was not changed, it maintained the lower power for the duration of the imaging session. This model of laser was clearly designed to favor maximum power rather than reproducibility. As another example of laser instability, Fig. 9f shows continual variations in laser intensity of >12% for a 488-nm laser on a four-laser CLSM system, adding a 12% uncertainty on all intensity measurements. This type of fluctuation, which requires a rarely performed time-series power measurement to detect, is common as diode lasers age, but can also occur on new lasers. Finally, Fig. 9g shows how the output power of the same laser line (488 nm) can vary tremendously between CLSMs. All of these fluctuations and intensity changes, undetected by the user, will prevent meaningful, quantitative comparisons from one system to the next, from one day to the next, or even from the start to the end of a single imaging session. Thus, regular quality control sessions and good test standards are currently required for rigorous quantification. Since most users do not have access to a power meter, or the time and/or expertise to remove the sample and check frequently for power fluctuations (particularly impossible during a time-lapse session), there is a need for more convenient, and preferably automated, ways to measure and monitor the power of each laser. Manufacturers should be encouraged to incorporate optical sensors into confocal microscope scanheads and provide real-time closed-loop feedback to maintain steady laser powers during an imaging session. Finally, the microscopy community should push manufacturers to move away from relative percent-laser-power numbers in confocal software and instead to provide true laser power measurements (mW), or even better, sample irradiance (illumination density) in W/m^2 within the CLSM software. This will enable the confocal community to establish guidelines for reasonable irradiance values under various experimental conditions (fixed cells, live cells, etc.) that can be easily applied across microscope types and vendors.

Problem number 4: 'jitter' and stripes

Since there are many sources of jitter and stripes in confocal microscope images, it can be difficult to determine the cause. Moreover, depending on the labeling, it may not be obvious that there is a problem at all. Linear structures such as actin filaments can help to reveal jitter, as shown in Fig. 9h where a CLSM image (Molecular Probes Prepared Slide #1, Thermo Fisher) is degraded by the bi-directional scanning feature (note that the jitter is worse to the left of the image and not apparent on the right side). Figure 9i shows stripes in a CLSM image of a uniform fluorescent slide (Chroma), caused by a defective Acousto-Optic Tuneable Filter (AOTF) driver. Several potential sources of jitter and stripes are as follows:

- Vibrations: Check that the optical table is floating properly, and avoid leaning on or bumping the table during acquisition. Ensure that there is no hardware on the table that could cause vibrations (e.g., bubbling humidifier bottles or power supplies with fans).
- Bi-directional scanning: When bi-directional scanning is used, re-calibration should be performed at the start of every session. On some CLSMs, it is impossible to remove the resulting jitter across the entire field of view—for these instruments, use bi-directional scanning only when the increased acquisition speed is necessary.
- Loose microscope component (e.g., stage or objective lens).
- Wiring (e.g., power cables) with tension on them sitting or pulling on the table or components.
- Stray room light: Although the confocal pinhole blocks out-of-focus light, including dim room light, stripes and/or background may arise from stray room light when using particularly sensitive techniques, such as two-photon microscopy with non-descanned detectors or pillar-mounted transmitted-light detectors. The alternating current that drives room lights shows up at 50–60-Hz intensity fluctuations. Try turning the room lights down/off and dimming/ turning off the computer monitor.
- Hardware problems: Fluctuations in the laser itself, noise due to the AOTF (or AOTF driver) or electronic noise picked up by the

Fig. 9 | Unexpected instrumentation issues cause uncertainty in intensity measurements. a, Fixed BPAE cells (Fluocells Prepared Slide #1, Thermo Fisher Scientific) imaged on a CLSM at the maximum field of view (zoom: 0.7) using a 20×/1.0 NA water immersion objective lens. The corners of the image appear darker than the center. **b**, By replacing the cells with a uniform plastic fluorescent slide (Chroma), the illumination non-uniformity can be measured (a 'shading reference' or 'flat-field' image) and potentially corrected. **c**, After plotting a line profile along the dashed line in **b**, the extent of the non-uniformity is now more obvious: there is a 60% change in intensity from the corner to the middle of the field at the lowest zoom (zoom 0.7), and still a 40% change at zoom 1. **d**, Focus drift measured on a new CLSM over several hours, revealing a widespread problem on confocal microscopes: within the first hour of powering on the microscope stand, the built-in focus drifts by >1 µm every 10 min. **e**, The 1-h warmup routine of one model of femtosecond laser; this routine was designed to maximize the power available to the user rather than favor reproducibility. **f**, Laser power as a function of time on a heavily used CLSM for the first 2 h after turning the instrument on. Users (as well as facility staff) were unaware that the most popular laser line (488-nm diode laser) was fluctuating by ~12% continually. **g**, The power of the 488-nm laser line across nine CLSMs, as measured at the specimen plane through a 10× objective (with the laser fixed in the center of the field of view rather than scanning). The power varies 50-fold between instruments. Also, bars B1 and B2 show a twofold change in power after replacing a laser on the same system. **h**, CLSM image of actin filaments caused by the bi-directional scanning feature. Note that the jitter is worse to the left of the image and not apparent on the right side. **i**, Stripes in an image of a uniform Chroma slide, caused by a defective AOTF driver. Scale bars = 50 µm (**a** and **b**); 2 µm (**h** and **i**).

detectors can all result in jitter or stripes. The microscope can be surrounded with a Faraday cage (wire mesh) to remove electronic noise. If these hardware problems cannot be resolved, call the microscope service engineers.

Analyzing and presenting quantitative images

Having spent considerable effort acquiring quantitative confocal images, it is essential to process and analyze the images in a manner that does not compromise their integrity. Although

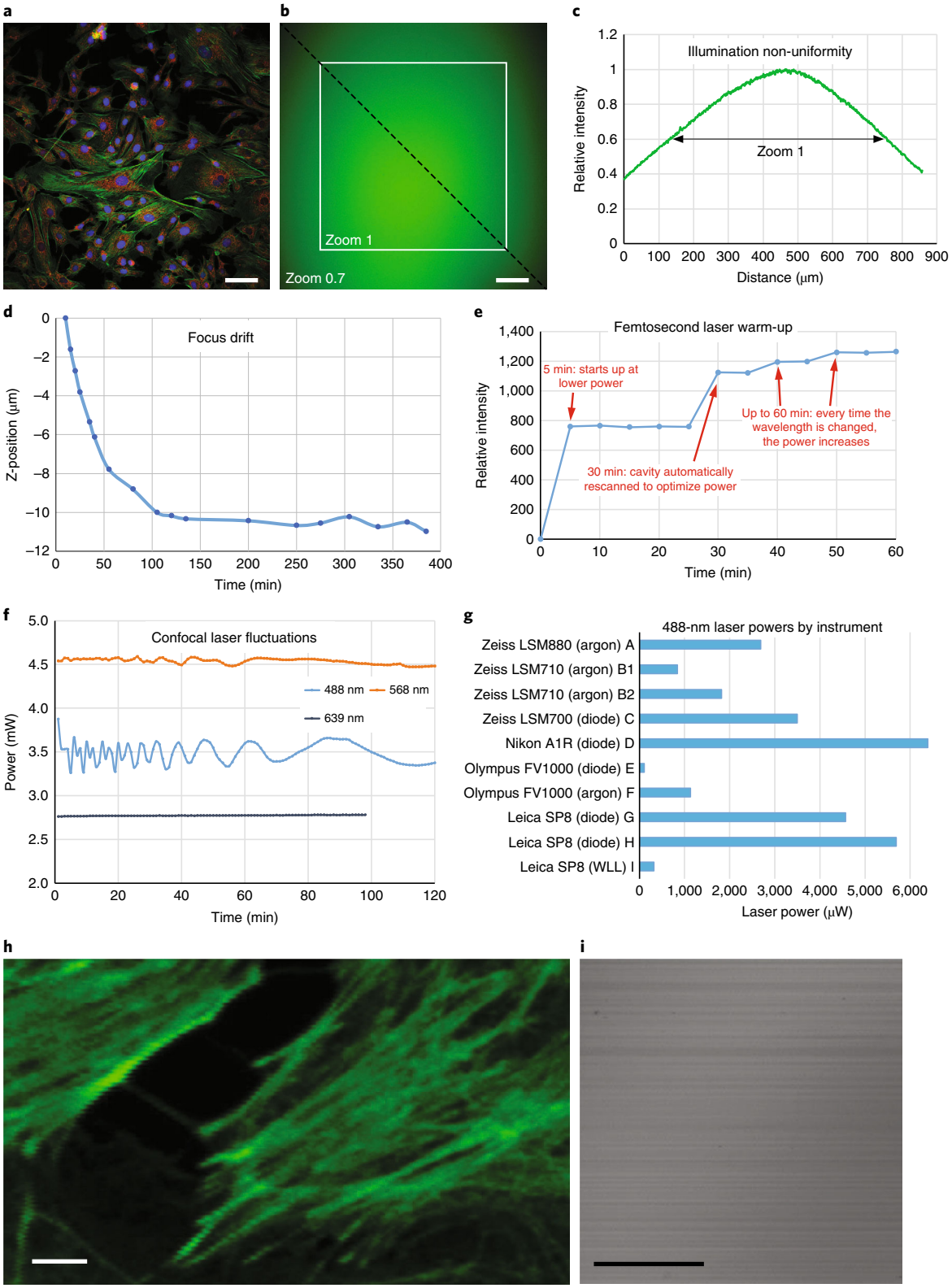

the confocal vendor's acquisition software may include image processing and analysis features (with various degrees of sophistication), most users turn to comprehensive third-party software. ImageJ is the most widely used open-source solution, including a variant called Fiji (Fiji Is Just ImageJ) that incorporates many popular plugins and additional documentation (https://fiji.sc/)[74,75]. Fiji is available on all common operating systems, and thanks to the integrated BioFormats Importer, it reads and displays most proprietary image formats and metadata. Metadata is important information about how an image was acquired (such as the objective lens used, pixel size and exposure time, details of the fluorescence channel, etc.) that is often required for quantitative analysis of the data[76]. Fiji can display multiple channels individually, as a composite or split out into separate image windows. Timeseries and z-stacks are treated as a series (called 'stacks' or 'hyperstacks') in a single window, with a slider to move between the individual dimensions of the images. From filtering (e.g., Gaussian smoothing) to thresholding (including 17 auto-thresholding algorithms), to measuring areas and intensities of objects ('Analyze Particles'), Fiji has the basics covered and much more. Fiji's open source architecture has led to the creation of hundreds of plugins by the community of users, including sophisticated ones such as Trainable Weka Segmentation[77] (using texture and machine learning to select and classify tissues or cells) and Trackmate[78] (automated, semi-automated and manual tracking of single particles). Repetitive processing and analysis steps can be automated using macros with minimal programming proficiency required: simply record new macro commands while analyzing one image, and then edit and run the macro on subsequent images. To get started with Fiji, refer to Arena et al[75], search the internet for online tutorials (e.g., https://imagej.net/Category:Tutorials) and/or consult staff at your local microscopy core facility.

CellProfiler (https://cellprofiler.org/)[79] is another freeware analysis program, specifically tailored to quantifying cell phenotypes[80]. CellProfiler helps users create and execute analysis 'pipelines', or sets of commands that are applied to entire groups of images. This can be particularly helpful for large volumes of images, such as those generated in high-content screening experiments.

Working with analysis pipelines can help ensure reproducible results: all images are necessarily processed identically, and the pipeline itself can be saved and scrutinized by supervisors, peers, collaborators and manuscript reviewers. A cloud-based version of CellProfiler called 'Distributed-CellProfiler' allows users to run analysis on thousands of images in parallel on Amazon Web Services (https://github.com/CellProfiler/Distributed-CellProfiler). The National Institute of Measurement Standards in the United States has developed the cloud-based Web Image Processing Pipelines (https://github.com/usnistgov/WIPP) for users and algorithm developers to work together to build and execute image analyse processes for TB-sized microscopy image data sets. Similarly, commercial versions of cloud-based analysis pipelines that allow the combination of several image analysis steps/algorithms/software packages into one workflow (including ImageJ plugins and macros) are also beginning to emerge, including Apeer (Zeiss, https://www.apeer.com/) and Knime (https://www.knime.com/), which are free for academic use. Cloud-based analysis platforms may be the best way to access computationally intensive new deep-learning algorithms for image restoration, such as de-noising and deconvolution, of fluorescence microscopy datasets[81,82].

The programming language Python is widely used for image analysis, and the Python image processing code library 'scikit Image' (https://scikit-image.org/) is a rapidly developing resource with >285 contributing developers and 14,000 packages that depend on it. Although Python requires significant programming expertise, platforms like Web Image Processing Pipelines and Apeer provide a resource to implement and test existing Python algorithms, integrate them into image analysis workflows and share these workflows with the broader community. Specific Python Tools for microscopy are being developed such as Python microscopy (https://python-microscopy.org/), cellular analysis (https://pypi.org/project/pySpacell/) and napari, a fast, interactive, multi-dimensional image viewer (http://napari.org). Together, these resources will accelerate the development and dissemination of tools available for image analysis and the integration of machine learning and artificial intelligence (AI) resources that are accessible for typical life science researchers to streamline workflows and advance quantitative imaging for the entire field.

Some analysis tasks are not very convenient (or even possible) in ImageJ or CellProfiler. For 3D rendering and analysis, there are some Fiji plugins, including ClearVolume[83] and GIANI (https://github.com/djpbarry/Giani/wiki), that may suffice. However, depending on the application, more powerful commercial solutions, such as Imaris (Oxford Instruments), Amira (Thermo Fisher Scientific), Vision 4D (Arivis), Aivia (DRVISION) or Volocity (Quorum Technologies), may be more appropriate. The commercial platforms harness the full power of modern computers and graphics cards, including graphics processing unit (GPU) processing and acceleration. For imaging and analyzing large tissue sections, dedicated digital pathology software, such as Halo (Indica Labs), VisioPharm, or the new freeware QuPath[63], may be more appropriate than Fiji. These programs can handle huge tiled-and-stitched (or scanned) images efficiently. They have integrated machine learning classifiers to segment the tissues into types (such as tumor versus stroma) by the textures and patterns in the tissues rather than just intensity thresholds, and after classification, there are algorithms for quantifying nuclear, cytoplasmic and membrane labeling of cells among other metrics.

Regardless of the software and kind of analysis to be performed, here are some key tips to maintain the integrity of a quantitative comparison[84,85]:

1 Always save the original, un-manipulated image and metadata in the microscope vendor's file format. If images are converted to TIFF format, the accompanying metadata may be lost unless you specifically use the BioFormats Open Microscopy Environment–TIFF format, developed by the Open Microscopy Environment consortium (http://openmicroscopy.org). JPEG images are suitable for presentations, but their lossy compression make them unsuitable for image analysis.

2 All images that are to be qualitatively (visually) compared must be processed using the exact same steps. For example, images should be displayed using the same contrast settings (typically raising the black level and lowering the white level).
3 All images that are to be quantitatively analyzed should also be processed identically. For example, apply the same threshold to all images when selecting positive cells for analysis. Alternatively, use the same auto-threshold algorithm for each image as a way of compensating for variations in background levels.
4 Non-linear contrast enhancement such as gamma, which treats dim and bright objects differently, must be used carefully and described in the figure legend.
5 Do not selectively edit one part of an image (e.g., brushing out a cell you do not like or lowering the intensity for just one region of an image).
6 Touching up images with photo editing tools (such as Adobe Photoshop) is generally forbidden: the blemishes are also part of the data.
7 Confocal images are often noisy. Linear smoothing filters (such as the Gaussian low-pass filter) can be helpful (and are usually appropriate) before analysis or presentation.
8 Deconvolution can enhance 3D datasets (they have little effect on 2D images) by removing noise, boosting contrast and improving resolution[40,86]. Use only rigorous image restoration algorithms, of which there are many kinds. Third-party programs such as Huygens deconvolution (Scientific Volume Imaging) have algorithms specifically optimized for different kinds of microscopes (CLSM, SD, multi-photon, Airyscan, STED, etc.), which may perform better than generic algorithms. Adjusting the deconvolution parameters appropriately (particularly the Point Spread Function (PSF), SNR and background estimates, which have a profound effect on the outcome) takes some experience. For quantitative results, the same parameters should be applied across all images. Avoid using deconvolution on undersampled images, and watch for artifacts such as mottled or speckled patterns.
9 All raw and processed images should be safely archived for a number of years (typically 5–10) according to the policies of your institution, funding agencies and the journal in which the results are published. Rather than (or in addition to) caring for a set of external hard drives, ask whether your institute offers a server running OMERO (https://www.openmicroscopy.org/omero/), an open source image database developed by an international team led by the University of Dundee[87]. You might also consider contributing your confocal microscopy data to public repositories such as the BioImage Archive[88] (https://www.ebi.ac.uk/bioimage-archive/).

Statistics

When performing quantitative confocal imaging, it is important to determine at what point there are sufficient data to determine if there are statistically significant differences. Several good reviews on this topic are available[89,90], and *Nature* has a collection of short articles called 'Statistics for Biologists' (https://www.nature.com/collections/qghhqm). General guidelines are presented here using a specific example of imaging adhesion dynamics within cells. Adhesions are dynamic structures that act as traction points for cells, and they form, grow and disassemble as the cell migrates. They can have many different sizes, shapes and dynamics (Fig. 10a). In this example, the rate of adhesion assembly was calculated by measuring adhesion intensities over 10–30 min for multiple adhesions from multiple cells[91].

It is important to repeat any experiment multiple times (i.e., experimental replicates) and ensure that the results are reproducible. Experiments should be repeated on different days and with all steps being independent between the replicates. Here, each experiment consisted of adhesion assembly measurements on 10 individual adhesions from each of three cells. The experiment was repeated three times, giving a total of 90 measured adhesions from nine cells. Even with 30 adhesions measured for each experiment, variation within the experiment can be high (Fig. 10b) (40% in this case), so three experimental replicates would be a minimum. Technical replicates are also important and consist of preparing the exact same sample multiple times in a single experimental run. This could mean making three identically stained coverslips with cells plated, fixed and stained at the same time. Technical replicates are important for checking on consistency in sample preparation and can detect errors such as pipette errors. Technical replicates should never be used to replace experimental replicates. Technical replicates were not performed in the adhesion example presented here.

Biological systems inherently show significant variability, hence the current boom in single-cell analysis. Measuring many cells at once determines average behavior, while single-cell data reveal subpopulations, outliers and interesting changes in underlying population distributions. Here, the cell-to-cell variation in adhesion assembly rates was high at 45%, while the variation between adhesion assembly rates within individual cells was only 35% (Fig. 10c).

The high variability in biological samples makes it important to measure many cells/tissue sections/animals for proper characterization. A minimum of 30 independent samples is generally recommended, but may be difficult to achieve for experimental systems such as mouse models. In the adhesion example, a total of 90 adhesion assembly rates was measured from nine cells (i.e., 10 adhesions per cell). Having measured just three adhesions would have been insufficient to characterize the population distribution (Fig. 10d), but as few as 10 adhesions still allowed a reasonable estimate of the mean and the median of the distribution, even though adhesions with faster assembly rates were not well represented. Thus, the difference between distributions across 30 or 90 adhesions would be important only for a more detailed analysis of subpopulations (Fig. 10d).

It is becoming more widely accepted that individual data points should be displayed and overlayed on box plots (Fig. 10d), rather than presented simply as bar graphs (Fig. 10e)[92]. Figure 10d,e clearly shows how the box plot gives the reader the ability to judge the quality and quantity of the experimental data directly, as well as plainly revealing outliers and clusters of data points within the distribution. Outliers should never be omitted from a box plot unless there is a flaw in the data collection or analysis, in which case formal tests to reject outliers should be applied[89].

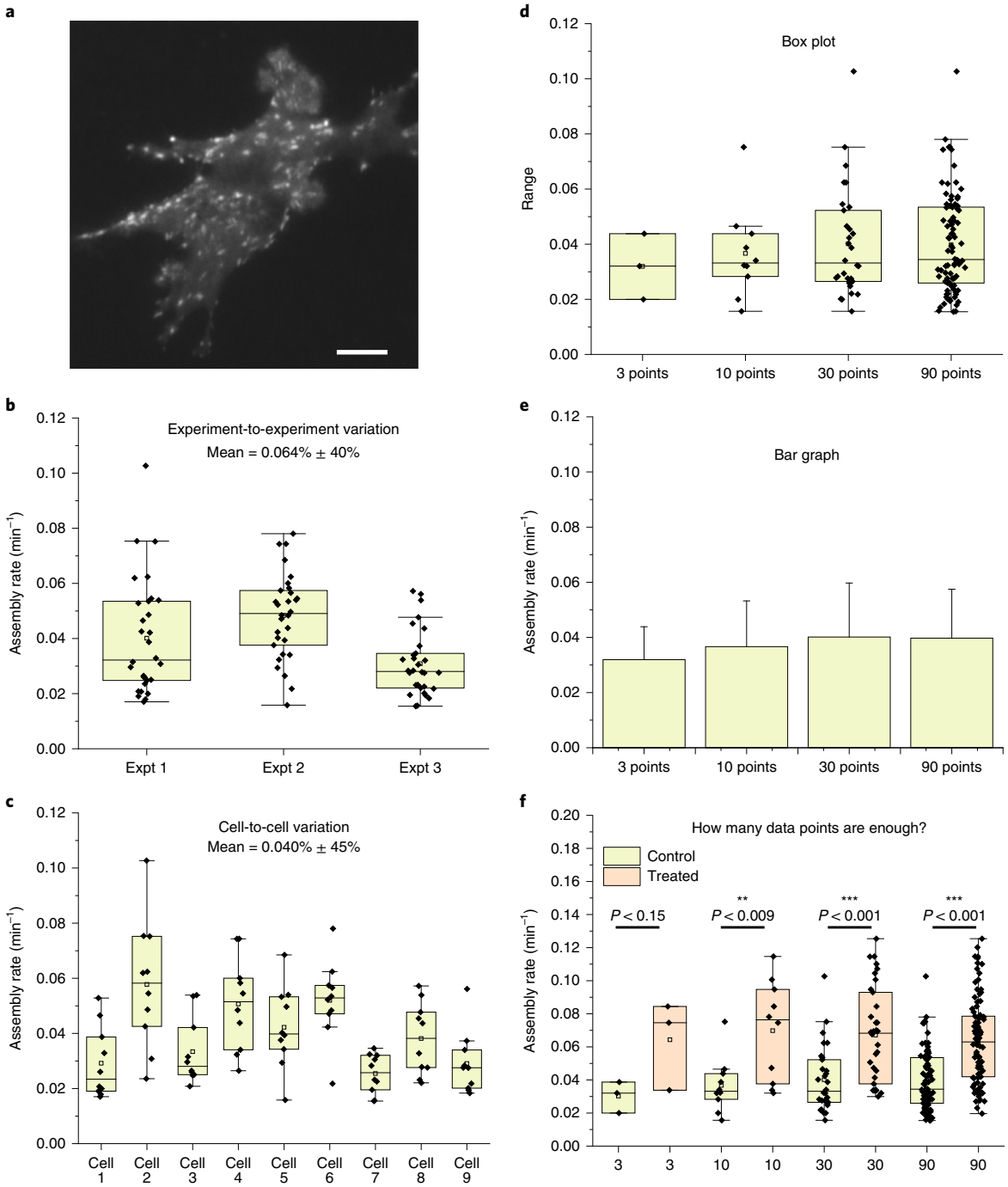

Fig. 10 | Sampling and statistics. a, Fluorescence image of eGFP-tagged protein localized to adhesion structures in NMuMG cells (ATCC, cat. no. CRL-1636, CVCL_0075). Scale bar = 10 μm. **b**, Adhesion assembly rates were calculated for 10 adhesions from each of three cells for a total of 30 in each of three independent experiments. Data for each experiment (Expt 1 to 3) are shown as a box plot. The line equals the median, the small open square equals the mean, the upper bar equals the 75th percentile and the bottom bar equals the 25th percentile of the distribution. Due to inherent biological variation, it is expected that variability between the three experiments is high (s.d. = 40%). **c**, Box plot of adhesion assembly rates for 10 adhesions from each of nine different cells. Inherent biological variation and variation between adhesion dynamics lead to high variation (s.d. = 45%). **d** and **e**, Box plot (**d**) and bar graph (**e**) of adhesion assembly rates from 3, 10, 30 or 90 adhesions. Comparison shows the importance of using box plots showing individual data points, and statistical information is much more informative than simple bar graphs. The box plot shows that 3 data points cannot clearly represent the entire sample distribution, 10 points begins to show the distribution and ≥30 points are ideal for characterizing the entire distribution. **f**, A second set of cells was treated with growth factor that increases adhesion assembly rates. Two-tailed, unequal-variance *t* test shows that even with 10 data points, the treatment leads to a statistically faster mean adhesion assembly rate with >95% confidence, while 30 or 90 data points lead to >99.9% confidence that the means of the two distributions are not the same.

The number of data points collected for a given experiment becomes particularly important when trying to assess whether two data sets are significantly different (Fig. 10f). The adhesion example shows assembly rates for control versus treated cells (growth factor treatment). Data are entered into a spreadsheet or scientific graphing package that performs statistical analyses. Researchers typically use a *t* test for this analysis and calculate the probability, *P*, that the difference between the means of the two data sets (e.g., control and treated) is due only to random chance[93]. A *P* value of <0.05 means that if the experiment was repeated 100 times, it is likely that five of those experiments gave you the wrong answer (i.e., there is a 5% probability that the means of the data sets are not different). In general, $P < 0.05$ is considered significant for biological systems with high variability, but it is recommended to have $P < 0.01$ to be more confident that there is a difference. Confidence can be displayed with an indication of the number of asterisks for a comparison of two data sets, to aid the reader in determining whether they agree with the experimental conclusions (Fig. 10f). Convention uses * for $P < 0.05$, ** for $P < 0.01$ and *** for $P < 0.001$. On the other hand, an increasing number of statisticians are asking researchers to simply report the *P* values and not make claims of statistical significance, as any chosen cut-off is somewhat arbitrary[94].

The number of data points, *n*, plays a big role in the *P* value calculation, leading to debate concerning the optimal value for *n*. In general, the choice of the *n* value and the *P* threshold for statistical significance depends on how confident the researcher wants to be in their conclusions. In the example given here, *n* could be 3 for the number of experiments, 9 for the number of cells, or 90 for the number of adhesions. The *P* value using $n = 90$ adhesions was <0.001, $P < 0.001$ for $n = 9$ cells and $P < 0.05$ for $n = 3$ experiments. Thus, even being cautious and using $n = 3$ experiments, there is a significant difference between the control and treated conditions.

When the means of the control and treated samples were compared for measurements of $n = 3$, 10, 30 or 90 adhesions (using n = number of adhesions), the differences were not significant for only 3 adhesions each (control and treated), were significant with 99% confidence for 10 adhesions and were significant with 99.9% confidence for 30 or 90 adhesions. Therefore, 30 adhesions for each condition was considered the optimal number for this experiment.

Concluding remarks

Is 'quantitative confocal microscopy' an oxymoron? The more experience you have with confocal imaging, the more you realize just how many things can go wrong. Indeed, several experts in the field have opined that it is nearly impossible to obtain rigorous measurements of intensities in a confocal experiment. Yet, no reviewer will accept qualitative comparisons between microscopy images: you will most likely be asked to quantify them! This tutorial should provide you with the tools to do this.

The primary responsibility for rigor and reproducibility in confocal microscopy rests with the experimenter. However, core facility staff and microscope manufacturers can also play critical roles. Core facility staff should be allowed the time and provided with the resources to perform regular quality control sessions on the instruments, at a minimum measuring laser powers, cleaning objectives and using a familiar, prepared slide to identify problems[70,95]. Confocal microscope users, developers and manufacturers have historically worked well together to design important new tools, but they must also partner to identify and develop methods and standards that will make reproducibility more inherent to all systems. Only then can truly quantitative data be achieved routinely throughout the confocal imaging community.

Reporting Summary

Further information on research design is available in the Nature Research Reporting Summary linked to this article.

References

1. Pawley, J. The 39 steps: a cautionary tale of quantitative 3-D fluorescence microscopy. *Biotechniques* **28**, 884–886 (2000). 888.
2. North, A. J. Seeing is believing? A beginners' guide to practical pitfalls in image acquisition. *J. Cell Biol.* **172**, 9–18 (2006).
3. Hell, S., Reiner, G., Cremer, C. & Stelzer, E. H. K. Aberrations in confocal fluorescence microscopy induced by mismatches in refractive index. *J. Microsc.* **169**, 391–405 (1993).
4. Richardson, D. S. & Lichtman, J. W. Clarifying tissue clearing. *Cell* **162**, 246–257 (2015).
5. Allan, V. J. Basic immunofluorescence. in *Protein Localization by Fluorescence Microscopy: A Practical Approach* (ed. Allan, V. J.) 1–26 (Oxford University Press, 1999).
6. McDonald, K. L., Morphew, M., Verkade, P. & Muller-Reichert, T. Recent advances in high-pressure freezing: equipment- and specimen-loading methods. *Methods Mol. Biol.* **369**, 143–173 (2007).
7. North, A. J., Chidgey, M. A., Clarke, J. P., Bardsley, W. G. & Garrod, D. R. Distinct desmocollin isoforms occur in the same desmosomes and show reciprocally graded distributions in bovine nasal epidermis. *Proc. Natl Acad. Sci. USA* **93**, 7701–7705 (1996).
8. Burry, R. W. *Immunocytochemistry: A Practical Guide for Biomedical Research* (Springer, 2010).
9. Park, Y. G. et al. Protection of tissue physicochemical properties using polyfunctional crosslinkers. *Nat. Biotechnol.* **37**, 73–83 (2019).
10. Richter, K. N. et al. Glyoxal as an alternative fixative to formaldehyde in immunostaining and super-resolution microscopy. *EMBO J.* **37**, 139–159 (2018).
11. Melan, M. A. & Sluder, G. Redistribution and differential extraction of soluble proteins in permeabilized cultured cells. Implications for immunofluorescence microscopy. *J. Cell Sci.* **101**(Pt 4), 731–743 (1992).
12. Jamur, M. C. & Oliver, C. Permeabilization of cell membranes. *Methods Mol. Biol.* **588**, 63–66 (2010).
13. Yan, Q. & Bruchez, M. P. Advances in chemical labeling of proteins in living cells. *Cell Tissue Res.* **360**, 179–194 (2015).
14. Ries, J., Kaplan, C., Platonova, E., Eghlidi, H. & Ewers, H. A simple, versatile method for GFP-based super-resolution microscopy via nanobodies. *Nat. Methods* **9**, 582–584 (2012).
15. Dolman, N. J., Kilgore, J. A. & Davidson, M. W. A review of reagents for fluorescence microscopy of cellular compartments and structures, part I: BacMam labeling and reagents for vesicular structures. *Curr. Protoc. Cytom.* **65**, 12.30.1–12.30.27 (2013).
16. Kilgore, J. A., Dolman, N. J. & Davidson, M. W. A review of reagents for fluorescence microscopy of cellular compartments and structures, Part II: reagents for non-vesicular organelles. *Curr. Protoc. Cytom.* **66**, 12.31.1–12.31.24 (2013).

17. Bordeaux, J. et al. Antibody validation. *Biotechniques* **48**, 197–209 (2010).
18. Pauly, D. & Hanack, K. How to avoid pitfalls in antibody use. *F1000Res* **4**, 691 (2015).
19. Stadler, C. et al. Systematic validation of antibody binding and protein subcellular localization using siRNA and confocal microscopy. *J. Proteomics* **75**, 2236–2251 (2012).
20. Stack, R. F. et al. Quality assurance testing for modern optical imaging systems. *Microsc. Microanal.* **17**, 598–606 (2011).
21. Cordes, T., Maiser, A., Steinhauer, C., Schermelleh, L. & Tinnefeld, P. Mechanisms and advancement of antifading agents for fluorescence microscopy and single-molecule spectroscopy. *Phys. Chem. Chem. Phys.* **13**, 6699–6709 (2011).
22. Piterburg, M., Panet, H. & Weiss, A. Photoconversion of DAPI following UV or violet excitation can cause DAPI to fluoresce with blue or cyan excitation. *J. Microsc.* **246**, 89–95 (2012).
23. Frigault, M. M., Lacoste, J., Swift, J. L. & Brown, C. M. Live-cell microscopy—tips and tools. *J. Cell Sci.* **122**, 753–767 (2009).
24. Ettinger, A. & Wittmann, T. Fluorescence live cell imaging. *Methods Cell Biol.* **123**, 77–94 (2014).
25. Lambert, T. J. FPbase: a community-editable fluorescent protein database. *Nat. Methods* **16**, 277–278 (2019).
26. Ai, H. W., Baird, M. A., Shen, Y., Davidson, M. W. & Campbell, R. E. Engineering and characterizing monomeric fluorescent proteins for live-cell imaging applications. *Nat. Protoc.* **9**, 910–928 (2014).
27. Rodriguez, E. A. et al. The growing and glowing toolbox of fluorescent and photoactive proteins. *Trends Biochem. Sci.* **42**, 111–129 (2017).
28. Cranfill, P. J. et al. Quantitative assessment of fluorescent proteins. *Nat. Methods* **13**, 557–562 (2016).
29. Bottanelli, F. et al. Two-colour live-cell nanoscale imaging of intracellular targets. *Nat. Commun.* **7**, 10778 (2016).
30. Erdmann, R. S. et al. Labeling strategies matter for super-resolution microscopy: a comparison between HaloTags and SNAP-tags. *Cell Chem. Biol.* **26**, 584–592.e6 (2019).
31. Wang, L. et al. A general strategy to develop cell permeable and fluorogenic probes for multicolour nanoscopy. *Nat. Chem.* **12**, 165–172 (2019).
32. Grimm, J. B., Brown, T. A., English, B. P., Lionnet, T. & Lavis, L. D. Synthesis of Janelia Fluor HaloTag and SNAP-Tag ligands and their use in cellular imaging experiments. *Methods Mol. Biol.* **1663**, 179–188 (2017).
33. Ferrando-May, E. et al. Advanced light microscopy core facilities: balancing service, science and career. *Microsc. Res. Tech.* **79**, 463–479 (2016).
34. Kiepas, A., Voorand, E., Mubaid, F., Siegel, P. M. & Brown, C. M. Optimizing live-cell fluorescence imaging conditions to minimize phototoxicity. *J. Cell Sci.* **133**, jcs242834 (2020).
35. Laissue, P. P., Alghamdi, R. A., Tomancak, P., Reynaud, E. G. & Shroff, H. Assessing phototoxicity in live fluorescence imaging. *Nat. Methods* **14**, 657 (2017).
36. Jonkman, J. E., Swoger, J., Kress, H., Rohrbach, A. & Stelzer, E. H. Resolution in optical microscopy. *Methods Enzymol.* **360**, 416–446 (2003).
37. Jacques, S. L. Optical properties of biological tissues: a review. *Phys. Med. Biol.* **58**, R37–R61 (2013).
38. Bolte, S. & Cordelieres, F. P. A guided tour into subcellular colocalization analysis in light microscopy. *J. Microsc.* **224**, 213–232 (2006).
39. Dunn, K. W., Kamocka, M. M. & McDonald, J. H. A practical guide to evaluating colocalization in biological microscopy. *Am. J. Physiol. Cell Physiol.* **300**, C723–C742 (2011).
40. Wallace, W., Schaefer, L. H. & Swedlow, J. R. A workingperson's guide to deconvolution in light microscopy. *Biotechniques* **31**, 1076–1078 (2001). 1080, 1082 passim.
41. Jonkman, J. & Brown, C. M. Any way you slice it—a comparison of confocal microscopy techniques. *J. Biomol. Tech.* **26**, 54–65 (2015).
42. Korobchevskaya, K., Lagerholm, B. C., Colin-York, H. & Fritzsche, M. Exploring the potential of Airyscan microscopy for live cell imaging. *Photonics* **4**, 41 (2017).
43. Zipfel, W. R., Williams, R. M. & Webb, W. W. Nonlinear magic: multiphoton microscopy in the biosciences. *Nat. Biotechnol.* **21**, 1369–1377 (2003).
44. Axelrod, D. Total internal reflection fluorescence microscopy in cell biology. *Traffic* **2**, 764–774 (2001).
45. Power, R. M. & Huisken, J. A guide to light-sheet fluorescence microscopy for multiscale imaging. *Nat. Methods* **14**, 360–373 (2017).
46. Strobl, F., Schmitz, A. & Stelzer, E. H. K. Improving your four-dimensional image: traveling through a decade of light-sheet-based fluorescence microscopy research. *Nat. Protoc.* **12**, 1103–1109 (2017).
47. Sigal, Y. M., Zhou, R. & Zhuang, X. Visualizing and discovering cellular structures with super-resolution microscopy. *Science* **361**, 880–887 (2018).
48. Wu, Y. & Shroff, H. Faster, sharper, and deeper: structured illumination microscopy for biological imaging. *Nat. Methods* **15**, 1011–1019 (2018).
49. Ishikawa-Ankerhold, H. C., Ankerhold, R. & Drummen, G. P. Advanced fluorescence microscopy techniques—FRAP, FLIP, FLAP, FRET and FLIM. *Molecules* **17**, 4047–4132 (2012).
50. Lippincott-Schwartz, J. & Patterson, G. H. Development and use of fluorescent protein markers in living cells. *Science* **300**, 87–91 (2003).
51. Lippincott-Schwartz, J., Altan-Bonnet, N. & Patterson, G. H. Photobleaching and photoactivation: following protein dynamics in living cells. *Nat. Cell Biol.* **Suppl**, S7–S14 (2003).
52. Elson, E. L. Fluorescence correlation spectroscopy: past, present, future. *Biophys. J.* **101**, 2855–2870 (2011).
53. Kim, S. A., Heinze, K. G. & Schwille, P. Fluorescence correlation spectroscopy in living cells. *Nat. Methods* **4**, 963–973 (2007).
54. Brown, C. M. et al. Raster image correlation spectroscopy (RICS) for measuring fast protein dynamics and concentrations with a commercial laser scanning confocal microscope. *J. Microsc.* **229**, 78–91 (2008).
55. Sprague, B. L. & McNally, J. G. FRAP analysis of binding: proper and fitting. *Trends Cell Biol.* **15**, 84–91 (2005).
56. Padilla-Parra, S. & Tramier, M. FRET microscopy in the living cell: different approaches, strengths and weaknesses. *Bioessays* **34**, 369–376 (2012).
57. Broussard, J. A., Rappaz, B., Webb, D. J. & Brown, C. M. Fluorescence resonance energy transfer microscopy as demonstrated by measuring the activation of the serine/threonine kinase Akt. *Nat. Protoc.* **8**, 265–281 (2013).
58. Bacia, K. & Schwille, P. Practical guidelines for dual-color fluorescence cross-correlation spectroscopy. *Nat. Protoc.* **2**, 2842–2856 (2007).
59. Krieger, J. W. et al. Imaging fluorescence (cross-) correlation spectroscopy in live cells and organisms. *Nat. Protoc.* **10**, 1948–1974 (2015).
60. Soderberg, O. et al. Direct observation of individual endogenous protein complexes in situ by proximity ligation. *Nat. Methods* **3**, 995–1000 (2006).
61. Holman, L., Head, M. L., Lanfear, R. & Jennions, M. D. Evidence of experimental bias in the life sciences: why we need blind data recording. *PLoS Biol.* **13**, e1002190 (2015).
62. Kaptchuk, T. J. The double-blind, randomized, placebo-controlled trial: gold standard or golden calf? *J. Clin. Epidemiol.* **54**, 541–549 (2001).
63. Bankhead, P. et al. QuPath: open source software for digital pathology image analysis. *Sci. Rep.* **7**, 16878 (2017).
64. Komura, D. & Ishikawa, S. Machine learning methods for histopathological image analysis. *Comput. Struct. Biotechnol. J.* **16**, 34–42 (2018).
65. Robertson, S., Azizpour, H., Smith, K. & Hartman, J. Digital image analysis in breast pathology—from image processing techniques to artificial intelligence. *Transl. Res.* **194**, 19–35 (2018).
66. Howard, V. & Reed, M. G. *Unbiased Stereology: Three-Dimensional Measurement in Microscopy* (Springer, 1998).

67. Kipanyula, M. J. & Sife, A. S. Global trends in application of stereology as a quantitative tool in biomedical research. *Biomed. Res. Int.* **2018**, 1825697 (2018).
68. Jonkman, J. E. et al. An introduction to the wound healing assay using live-cell microscopy. *Cell Adh. Migr.* **8**, 440–451 (2014).
69. Zimmermann, T., Marrison, J., Hogg, K. & O'Toole, P. Clearing up the signal: spectral imaging and linear unmixing in fluorescence microscopy. *Methods Mol. Biol.* **1075**, 129–148 (2014).
70. Jonkman, J., Brown, C. M. & Cole, R. W. Quantitative confocal microscopy: beyond a pretty picture. *Methods Cell Biol.* **123**, 113–134 (2014).
71. Oreopoulos, J., Berman, R. & Browne, M. Chapter 9—Spinning-disk confocal microscopy: present technology and future trends. in *Methods in Cell Biology: Quantitative Imaging in Cell Biology* Vol. **123** (eds Waters, J. C. & Wittman, T.) 153–175 (Academic Press, 2014).
72. Model, M. A. & Blank, J. L. Concentrated dyes as a source of two-dimensional fluorescent field for characterization of a confocal microscope. *J. Microsc.* **229**, 12–16 (2008).
73. International Organization for Standardization. *Microscopes—Confocal microscopes—Optical data of fluorescence confocal microscopes for biological imaging*. ISO Standard No. **21073:2019** (2019).
74. Schindelin, J. et al. Fiji: an open-source platform for biological-image analysis. *Nat. Methods* **9**, 676–682 (2012).
75. Arena, E. T. et al. Quantitating the cell: turning images into numbers with ImageJ. *Wiley Interdiscip. Rev. Dev. Biol.* **6**, e260 (2017).
76. Linkert, M. et al. Metadata matters: access to image data in the real world. *J. Cell Biol.* **189**, 777–782 (2010).
77. Arganda-Carreras, I. et al. Trainable Weka Segmentation: a machine learning tool for microscopy pixel classification. *Bioinformatics* **33**, 2424–2426 (2017).
78. Tinevez, J. Y. et al. TrackMate: an open and extensible platform for single-particle tracking. *Methods* **115**, 80–90 (2017).
79. McQuin, C. et al. CellProfiler 3.0: next-generation image processing for biology. *PLoS Biol.* **16**, e2005970 (2018).
80. Bray, M. A. et al. Cell Painting, a high-content image-based assay for morphological profiling using multiplexed fluorescent dyes. *Nat. Protoc.* **11**, 1757–1774 (2016).
81. Weigert, M. et al. Content-aware image restoration: pushing the limits of fluorescence microscopy. *Nat. Methods* **15**, 1090–1097 (2018).
82. Belthangady, C. & Royer, L. A. Applications, promises, and pitfalls of deep learning for fluorescence image reconstruction. *Nat. Methods* **16**, 1215–1225 (2019).
83. Royer, L. A. et al. ClearVolume: open-source live 3D visualization for light-sheet microscopy. *Nat. Methods* **12**, 480–481 (2015).
84. Cromey, D. W. Avoiding twisted pixels: ethical guidelines for the appropriate use and manipulation of scientific digital images. *Sci. Eng. Ethics* **16**, 639–667 (2010).
85. Cromey, D. W. Digital images are data: and should be treated as such. *Methods Mol. Biol.* **931**, 1–27 (2013).
86. Goodwin, P. C. Quantitative deconvolution microscopy. *Methods Cell Biol.* **123**, 177–192 (2014).
87. Allan, C. et al. OMERO: flexible, model-driven data management for experimental biology. *Nat. Methods* **9**, 245–253 (2012).
88. Ellenberg, J. et al. A call for public archives for biological image data. *Nat. Methods* **15**, 849–854 (2018).
89. Fay, D. S. & Gerow, K. A biologist's guide to statistical thinking and analysis. *WormBook* Jul 9, 1–54 (2013).
90. Vaux, D. L. Basic statistics in cell biology. *Annu. Rev. Cell Dev. Biol.* **30**, 23–37 (2014).
91. Lacoste, J., Young, K. & Brown, C. M. Live-cell migration and adhesion turnover assays. *Methods Mol. Biol.* **931**, 61–84 (2013).
92. Krzywinski, M. & Altman, N. Visualizing samples with box plots. *Nat. Methods* **11**, 119–120 (2014).
93. Krzywinski, M. & Altman, N. Significance, *P* values and *t*-tests. *Nat. Methods* **10**, 1041–1042 (2013).
94. Wasserstein, R. L., Schirm, A. L. & Lazar, N. A. Moving to a world beyond "$p < 0.05$". *Am. Stat.* **73**, 1–19 (2019).
95. Hibbs, A. R., MacDonald, G. & Garsha, K. Chapter 36: Practical confocal microscopy. in *Handbook of Biological Confocal Microscopy* 3rd edn (ed. Pawley, J. B.) (Springer, 2006).
96. Wang, H., Lacoche, S., Huang, L., Xue, B. & Muthuswamy, S. K. Rotational motion during three-dimensional morphogenesis of mammary epithelial acini relates to laminin matrix assembly. *Proc. Natl Acad. Sci. USA* **110**, 163–168 (2013).
97. Cole, R. W., Jinadasa, T. & Brown, C. M. Measuring and interpreting point spread functions to determine confocal microscope resolution and ensure quality control. *Nat. Protoc.* **6**, 1929–1941 (2011).

Acknowledgements

J.J. thanks the AOMF staff for helpful discussions, Courtney McIntosh for the images in Supplementary Fig. 1, and the Princess Margaret Foundation for ongoing financial support of the AOMF. G.D.W. thanks A*STAR and the National Research Foundation's Shared Infrastructure Support Grant for continued support of the A*STAR Microscopy Platform and John Common for samples (Box 2). C.M.B. acknowledges Alex Kiepas (McGill University), who collected the adhesion dynamics data for the statistics section of the paper including Fig. 10, and the ABIF for general support and access to the Diskovery spinning disk TIRF microscope for collecting the adhesion dynamics data. K.I.A. thanks the Francis Crick Institute for their CALM support, and facility colleagues for helpful discussion. A.J.N. thanks the Rockefeller University for its continued support of the Frits and Rita Markus Bio-Imaging Resource Center (BIRC), the Sohn Conference Foundation for funding the Leica SP8 confocal microscope used to generate Figs. 3 and 4 and the facility staff and users for stimulating discussions.

Author contributions

No section of this manuscript was untouched by all five authors. J.J. drafted the outline, assembled the team and wrote the Introduction, 'Removing bias', 'Troubleshooting instrumentation issues' and 'Analyzing and presenting quantitative images'. He also generated Figs. 1, 2, 6, 7, 8 and 9; Table 1; Box 3; and Supplementary Figs. 1 and 2 and contributed to general editing. C.M.B. analyzed adhesion dynamics data, generated the statistics figure (Fig. 10), wrote the Statistics section of the manuscript and contributed to 'General considerations for preparing samples for quantitative fluorescence microscopy', 'Preparing fixed cells and tissues' and 'Preparing live cells' and significantly to general editing of the manuscript. G.D.W. worked on 'Choosing the right microscope' and 'Setting up the microscope', performed general editing of the manuscript and generated Fig. 5, the images for Box 2 and Supplementary Video 1. K.I.A. worked on 'Choosing the right microscope' and 'Planning your experiment' and performed general editing of the manuscript. A.J.N. worked on 'General considerations for preparing samples for quantitative fluorescence microscopy' and 'Setting up the microscope', contributed extensively to general editing and generated Figs. 3 and 4 and Boxes 1 and 2.

Competing interests

The authors declare no competing interests.

Additional information

Supplementary information is available for this paper at https://doi.org/10.1038/s41596-020-0313-9.

Correspondence and requests for materials should be addressed to J.J.

Peer review information *Nature Protocols* thanks Gary Laevsky, Timo Zimmermann and the other, anonymous, reviewer(s) for their contribution to the peer review of this work.

Reprints and permissions information is available at www.nature.com/reprints.

Publisher's note Springer Nature remains neutral with regard to jurisdictional claims in published maps and institutional affiliations.

Received: 11 August 2019; Accepted: 10 February 2020;
Published online: 31 March 2020

Related links

Guidance for Quantitative Confocal Microscopy (https://doi.org/10.1038/s41596-020-0307-7): This poster is a visual summary of this paper.
Molecular Expressions Optical Microscopy Primer (https://micro.magnet.fsu.edu/primer/): Developed by Michael W. Davidson and his team at The Florida State University, this website hosts a vast amount of knowledge on all aspects of optical microscopy from the physics of light and color and the anatomy of a basic transmitted-light microscope to advanced techniques such as FRET and TIRF.
iBiology Microscopy Series (https://www.ibiology.org/online-biology-courses/microscopy-series/): Directed by Ron Vale, Nico Stuurman and Kurt Thorn, this 72-video series (and growing!) starts with the basics of optical microscopy and concludes with some of the latest techniques, such as super-resolution microscopy. Their Short Microscopy series of just 14 videos may be more manageable for some.
iBiology BioImage Analysis Course (https://www.ibiology.org/online-biology-courses/bioimage-analysis-course/): Created by Anne Carpenter (CellProfiler project lead) and Kevin Eliceiri (ImageJ project lead), this series focuses on general steps of image processing as well as introductions to CellProfiler and ImageJ specifically.
Microscope Vendor websites: Many microscope vendors have educational material on their websites. Some of them license sections from Molecular Expressions, but supplemented with their own microscopes' unique attributes. Others have written their own material from scratch.
The Confocal Microscopy Listserv (https://lists.umn.edu/cgi-bin/wa?A0=confocalmicroscopy): With an active subscriber base of nearly 4,000 participants and an archive that goes back to 1991, the Confocal Listserv is a valuable resource for confocal and related questions. Registration (free) is required.
Microforum (https://forum.microlist.org/): This new web forum led by Jennifer Waters and Tally Lambert was established in 2019. Its focus is on hardware, acquisition and specimen-related aspects of scientific imaging, particularly (but not limited to) the theory and practical use of optical microscopes and detectors, fluorescent proteins and probes and specimen preparation.

nature research

Corresponding author(s): James Jonkman

Last updated by author(s): Aug 12, 2019

Reporting Summary

Nature Research wishes to improve the reproducibility of the work that we publish. This form provides structure for consistency and transparency in reporting. For further information on Nature Research policies, see Authors & Referees and the Editorial Policy Checklist.

Statistics

For all statistical analyses, confirm that the following items are present in the figure legend, table legend, main text, or Methods section.

n/a	Confirmed	
☐	☒	The exact sample size (*n*) for each experimental group/condition, given as a discrete number and unit of measurement
☐	☒	A statement on whether measurements were taken from distinct samples or whether the same sample was measured repeatedly
☐	☒	The statistical test(s) used AND whether they are one- or two-sided *Only common tests should be described solely by name; describe more complex techniques in the Methods section.*
☒	☐	A description of all covariates tested
☒	☐	A description of any assumptions or corrections, such as tests of normality and adjustment for multiple comparisons
☒	☐	A full description of the statistical parameters including central tendency (e.g. means) or other basic estimates (e.g. regression coefficient) AND variation (e.g. standard deviation) or associated estimates of uncertainty (e.g. confidence intervals)
☒	☐	For null hypothesis testing, the test statistic (e.g. *F*, *t*, *r*) with confidence intervals, effect sizes, degrees of freedom and *P* value noted *Give P values as exact values whenever suitable.*
☒	☐	For Bayesian analysis, information on the choice of priors and Markov chain Monte Carlo settings
☒	☐	For hierarchical and complex designs, identification of the appropriate level for tests and full reporting of outcomes
☒	☐	Estimates of effect sizes (e.g. Cohen's *d*, Pearson's *r*), indicating how they were calculated

Our web collection on statistics for biologists contains articles on many of the points above.

Software and code

Policy information about availability of computer code

Data collection	Confocal microscopy images were collected with Leica LAS-X ver3.1 or Zeiss Zen (Black) Ver 2.3
Data analysis	3D image analysis (Figure 1) was performed using Imaris (Bitplane) ver 9.1. All other analysis (2D) was performed using Fiji ImageJ ver 1.52h.

For manuscripts utilizing custom algorithms or software that are central to the research but not yet described in published literature, software must be made available to editors/reviewers. We strongly encourage code deposition in a community repository (e.g. GitHub). See the Nature Research guidelines for submitting code & software for further information.

Data

Policy information about availability of data

All manuscripts must include a data availability statement. This statement should provide the following information, where applicable:

- Accession codes, unique identifiers, or web links for publicly available datasets
- A list of figures that have associated raw data
- A description of any restrictions on data availability

The data presented is for tutorial purposes only.

Field-specific reporting

Please select the one below that is the best fit for your research. If you are not sure, read the appropriate sections before making your selection.

☒ Life sciences ☐ Behavioural & social sciences ☐ Ecological, evolutionary & environmental sciences

Life sciences study design

All studies must disclose on these points even when the disclosure is negative.

Sample size	n/a
Data exclusions	n/a
Replication	n/a
Randomization	n/a
Blinding	n/a

Reporting for specific materials, systems and methods

We require information from authors about some types of materials, experimental systems and methods used in many studies. Here, indicate whether each material, system or method listed is relevant to your study. If you are not sure if a list item applies to your research, read the appropriate section before selecting a response.

Materials & experimental systems

n/a	Involved in the study
☒	☐ Antibodies
☒	☐ Eukaryotic cell lines
☒	☐ Palaeontology
☒	☐ Animals and other organisms
☒	☐ Human research participants
☒	☐ Clinical data

Methods

n/a	Involved in the study
☒	☐ ChIP-seq
☒	☐ Flow cytometry
☒	☐ MRI-based neuroimaging